Science Translational Medicine
AAAS

stm.sciencemag.org/cgi/content/full/11/495/eaav5597/DC1

Supplementary Materials for

Lymphocyte-driven regional immunopathology in pneumonitis caused by impaired central immune tolerance

Elise M. N. Ferré, Timothy J. Break, Peter D. Burbelo, Michael Allgäuer, David E. Kleiner, Dakai Jin, Ziyue Xu, Les R. Folio, Daniel J. Mollura, Muthulekha Swamydas, Wenjuan Gu, Sally Hunsberger, Chyi-Chia R. Lee, Anamaria Bondici, Kevin W. Hoffman, Jean K. Lim, Kerry Dobbs, Julie E. Niemela, Thomas A. Fleisher, Amy P. Hsu, Laquita N. Snow, Dirk N. Darnell, Samar Ojaimi, Megan A. Cooper, Martin Bozzola, Gary I. Kleiner, Juan C. Martinez, Robin R. Deterding, Douglas B. Kuhns, Theo Heller, Karen K. Winer, Arun Rajan, Steven M. Holland, Luigi D. Notarangelo, Kevin P. Fennelly, Kenneth N. Olivier, Michail S. Lionakis*

*Corresponding author. Email: lionakism@mail.nih.gov

Published 5 June 2019, *Sci. Transl. Med.* **11**, eaav5597 (2019)
DOI: 10.1126/scitranslmed.aav5597

The PDF file includes:

Other Supplementary Material for this manuscript includes the following:

(available at www.sciencetranslationalmedicine.org/cgi/content/full/11/495/eaav5597/DC1)

Data file S1 (Microsoft Excel format). Primary data.

Supplementary Materials and Methods

Non-contrast chest CT acquisition and scoring

Chest CT exams were performed on the Siemens Force or Flash (Siemens Health-care USA), Philips Brilliance (Philips Healthcare), Toshiba Aquillion ONETMVision CT (Toshiba MedicalSystems Corporation) or GE Lightspeed (GE MedicalSystems) using 0.6–2.5-mm collimation, 120 kVp, 150–240 reference mAs (with dose modulation), and 0.6–0.75-s rotation time. Images were pushed to our picture archiving and communication system (PACS, Carestream Health) as contiguous 5×5-mm and 2×1-mm overlap axial slices for coronal multiplanar and other reformats. Scans were obtained with patients coached to full inspiration, supine.

Blinded radiographic scoring, performed by the same radiologist to minimize operator bias, included the following 8 criteria: mosaicism, bronchiectasis, tree-in-bud, nodules, mucus plugs, GGO, air-space opacities, and cavitary lesions. Each criterion was assessed separately in both lungs with a score scale from zero to three per lung, where zero indicated the absence of the corresponding lesion, one indicated the presence of a mild lesion, 2 indicated the presence of a moderate lesion, and 3 indicated the presence of a severe lesion. The total possible score was 48.

Chest CT volumetric analysis and 3D Rendering

Volumetric analysis of CT scans was performed in a semi-automatic manner. First, a deep learning model was developed to automatically identify the potential areas of the

diseased lung regions in APECED patients. Then, an expert carefully went through all results and performed manual corrections to the automatic detected disease volumes.

For the first automatic step, the working pipeline included: lung segmentation (*48*), airway and pulmonary vessel segmentation (*49*), and disease region detection. We identified the diseased volumes from the CT scan using a deep convolutional neural network architecture, progressive holistic neural network (P-HNN) (*48-50*). The P-HNN model is trained using a public dataset from University Hospital of Geneva (*51*), which contains 17 types of interstitial lung disease patterns from 120 high-resolution CT scans. For this work, 6 types (including healthy) were used to train our P-HNN model to distinguish between healthy lung tissues against GGO, fibrosis, micro-nodule, consolidation, and pneumocystis pneumonia. Specifically, we fine-tuned our P-HNN using the initial network weights from ImageNet pre-trained VGG16 model (*52*). The training parameters includes: learning rate: '1e-8', Adam solver with momentum '0.9' and momentum2 '0.999'. The network has been trained ~10 epochs. We randomly split 85% data for training and 15% data for validation, and the accuracy is comparable to patch-based methods (*53*).

The final disease volumetric quantification was performed after removal of the normal airways and pulmonary vessels from the corrected disease volume. We use ITK-SNAP software (*54*) for the 3D rendering of the disease volumes and 3D rendering results.

Sputum induction

Sputum was induced with inhalation of 3% NaCl solution and evaluated by gram stain, wet mount, and routine respiratory, fungal, and mycobacterial cultures at the NIH Clinical Center Microbiology Laboratory.

Bronchoscopy with BAL harvesting and endobronchial biopsies

Bronchoscopy

Bronchoscopy was performed under an IRB-approved research protocol in 4 healthy volunteers and as clinically indicated in 5 APECED patients with active symptoms and/or radiographic abnormalities during their NIH visit. BAL was performed in adults with serial 30 mL aliquots of saline for a total instillation of 150 mL in each of the right middle lobe and lingula in healthy controls. In patients with APECED, the same volume was instilled in the lobe(s) with the greatest involvement. Lavage volumes for pediatric patients were administered in increments of 10 ml aliquots per ATS/ERS guidelines (*55*). BAL evaluations included cytologic evaluation and microbiologic studies and FACS analysis of immune cell subsets. Endobronchial biopsies were performed under direct visualization with disposable forceps in the anterior aspects of the proximal lobar and segmental airways. Endobronchial biopsies and previously-performed transbronchial and open lung biopsies requested from outside hospitals were evaluated by histology and immunohistochemistry.

Histological and immunohistochemical analyses

Endobronchial and deeper lung tissue samples (wedge biopsies, resection specimens, and an autopsy case) were routinely processed and sectioned at 5 μm for H&E and immunohistochemistry. Immunohistochemistry was performed at the NCI Laboratory of Pathology using the Ventana Benchmark XT (Ventana) on a Leica BOND-MAX (Leica Microsystems) automated immunostainer using manufacturer recommended antigen retrieval methods. The following antibodies were used: CD3 (2GV6, Ventana #790-4341, predilute), CD4 (SP35, Roche #790-4423, predilute), CD8 (CD8/144B, Dako #M7103, 1:25), and CD20 (L26, Roche #760-2531, predilute).

The specimens were assessed for the presence of inflammation. Lymphocytic infiltrates were assessed as minimal/close to normal, mild, moderate, and marked. If distinct patterns were present (e.g. increased intraepithelial lymphocytes, band-like infiltrates, organized follicular structures, or nodules/aggregates) those were described. Furthermore, the presence of squamous metaplasia and basement membrane thickening, both reactions to chronic irritation, were assessed. Slides were digitally scanned using an Aperio ScanScope XT (Leica Biosystems). In endobronchial biopsies, basement membrane thickness was measured in five different locations per specimen using QuPath (*56*).

BAL immunophenotyping using FACS

BAL was centrifuged and the supernatant stored at -80ºC. The pellet was resuspended in PBS to obtain a single cell suspension. BAL staining was performed using the following fluorochrome-conjugated (BV605, BV570, eFluor450, FITC, PE, PerCP-Cy5.5, PE-Cy7,

APC, AF700, APC-Cy7) antibodies against human CD45 (H130), CD19 (HIB19), CD3 (SK7 or OKT3), CD4 (RPA-T4), CD123 (6H6), CD56 (CMSSB), CD15 (MMA or HI98), CD11b (ICRF44), CD11c (3.9), CD25 (BC96), CD127 (RDR5), CD1c (L161), CD66b (G10F5), γδTCR (B1.1), CD206 (19.2) (eBioscience); CD16 (3G8), HLA-DR (G46-6), CD14 (M5E2 or MP9), CD63 (H5C6), CD18 (3G8) (BD Pharmingen); CD8 (HIT8a) (BioLegend); b558 (7D5) (MBL) for 30 minutes on ice. After incubation, the cells were washed with FACS buffer and the samples acquired using an LSR Fortessa (BD Biosciences). FlowJo was used for the final analysis. Cell numbers were quantified using PE-conjugated counting beads (Spherotech) (*56*). Neutrophils were defined as $SSC^{int}CD45^{+}CD15^{+}CD16^{+}CD11b^{+}HLA\text{-}DR^{-}$ cells; alveolar macrophages were defined as $SSC^{hi}CD45^{+}CD15^{-}HLA\text{-}DR^{+}$, which also expressed CD206, CD123 and CD11c; monocytes were defined as $SSC^{lo}CD45^{+}CD15^{-}HLA\text{-}DR^{+}CD14^{+}CD11b^{+}$; and $CD4^{+}$ T, $CD8^{+}$ T, γδ T, NK, NKT, and B cells were defined as $SSC^{lo}CD45^{+}$ cells expressing CD3/CD4, CD3/CD8, CD3/γδ TCR, CD56($CD3^{-}$), CD3/CD56 and CD19, respectively. Regulatory T cells were defined as $SSC^{lo}CD45^{+}CD3^{+}CD4^{+}CD127^{lo}CD25^{+}$.

Microbiology

Gram stain, wet mount, modified acid-fast stain, acid fast stain, bacterial, fungal, mycobacterial, *Nocardia*, and *Legionella* cultures were performed by the NIH Clinical Center Microbiology Laboratory. Qualitative real-time PCR amplification was employed for the detection of CMV, HSV-1, HSV-2, *Pneumocystis jirovecii* and *Legionella pneumophila* genomes using specific DNA probes. A FilmArray utilizing a real-time multiplexed PCR for the simultaneous qualitative detection and identification of multiple

respiratory viral and bacterial pathogens was employed to identify adenovirus, influenza A (subtype seasonal H1, subtype 2009 H1, or subtype H3), influenza B, parainfluenza viruses 1-4, respiratory syncytial virus, human metapneumovirus, coronavirus 229E, HKU1, NL63, and OC43, human rhinovirus/enterovirus, *Bordetella pertussis*, *Chlamydophila pneumoniae*, and *Mycoplasma pneumoniae*.

ELISA for human MPO and MMP-9

BAL supernatants were used to quantify MPO by the DuoSet ELISA kit and MMP-9 by the Quantikine ELISA kit (R&D systems) according to manufacturers' instructions.

***AIRE* sequencing**

DNA was harvested from whole blood for investigation of *AIRE* mutations by Sanger sequencing using two sets of primers that cover all 14 exons, highly-conserved intronic regions and 5'UTR and 3'UTR regions (*6*). Copy number variation was employed in patients without identified biallelic *AIRE* mutations using the exon-level oligo array CGH platform of GeneDX (*6*).

HLA sequencing

Genomic DNA was isolated from blood using the Qiagen BioRobot EZ1 and associated DNA isolation kits (Qiagen). Low/intermediate typing for Class I (A/B/C) and Class II loci (DRB1/DQB1/DRB345) was performed using LABType sequence-specific oligonucleotide (SSO) Typing Kits obtained from One Lambda, Inc. Target DNA was

amplified by PCR using a group-specific primer. The biotinylated PCR product was then detected using R-Phycoerythrin-conjugated Streptavidin (SAPE).

Some samples required the use of sequence-based typing (SBT) methodology to verify or further interpret the HLA type. SBT was performed utilizing a big dye terminator chemistry method. Primary PCR amplification using the HLA Sequenced Based Typing Kits (One Lambda) produced a 1.5 kb amplicon, and the products were purified from excess primers, dNTPs and genomic DNA using ExoSAP-IT (American Life Science). Each template was sequenced in the forward and reverse sequence orientation. Excess dye terminators were removed from the sequencing products utilizing an ethanol precipitation method with absolute ethanol. Reaction products were reconstituted with 15 μl of Hi-Di$_{TM}$ Formamide (PE Applied Biosystems/Perkin-Elmer) and analyzed on the Applied Biosystems (ABI) Prism*3730xL DNA Analyzer or the 3500xL DNA Analyzer.

Autoantibody detection

Luciferase immunoprecipitation systems (LIPS) assay

The LIPS immunoassay was used to detect autoantibody immunoreactivity against BPIFB1, KCNRG, tyrosine phosphatase-related islet antigen 2 (IA-2), tyrosine hydroxylase (TH), tryptophan hydroxylase (TPH), side chain cleavage enzyme (SCC), and NLR family and pyrin domain containing 5 (NALP5) in APECED patient sera (*6*). Seropositivity for these autoantibodies in APECED patients was calculated based on the mean plus three standard deviations of control patients as previously described (*6*).

Particle-based multiplex assay

A particle-based approach was used to detect immunoreactivity against Th17 cytokines, which was calculated based on the mean plus 3 standard deviations of the healthy donor control group as previously described (*6*).

Other methodologies

Autoantibody detection performed at the NIH Clinical Center Department of Laboratory Medicine included chemiluminescence for autoantibodies against thyroid peroxidase (TPO) and anti-thyroglobulin, immunoabsorption for autoantibodies against 21-hydroxylase, competitive binding immunoenzymatic assay for intrinsic factor blocking antibody, enzyme-linked immunosorbent assay for parietal cell IgG antibody, and radioimmunoassay for glutamic acid decarboxylase 65 (GAD65) antibodies (*6*).

Measurement of inflammatory markers and immunoglobulins

ESR and CRP were measured by the Modified Westergren Method and particle enhanced immunoturbidimetric assay, respectively, at the NIH Clinical Center Chemistry Laboratory.

Lymphocyte immunophenotyping from human blood using FACS

Whole blood harvested in EDTA tubes, was prepared by lysing red blood cells using BD FACS Lysing Solution, and stained with the following fluorochrome-conjugated (FITC, PE, PE-Cy7, APC, APC-eFluor 780, AF700, eFluor 450, PerCP-Cy5.5) antibodies against human CD45 (HI30), CD19 (SJ25C1), CD27 (TNFRSF7), CD10 (CB-CALLA) (eBioscience); CD3 (SK7), CD16 (SK7), CD56 (SK7), CD20 (L27), CD62L (SK11), CD38 (HB7) (BD Biosciences); IgM (MHM-88), CD21 (Bu32) (BioLegend); CD4 (S3.5), CD8 (3B5) (Thermo

Fisher Scientific); CD45RA (ALB11) (Beckman Coulter) for 30 minutes on ice. Following incubation, the cells were washed with FACS buffer, acquired using a FACSCanto (BD Biosciences), and analyzed using FlowJo (TreeStar). Patient's same-day absolute lymphocyte count was used to quantify cell numbers from the FACS plot percentages.

Mice

Aire$^{-/-}$ mice on the NOD background were purchased from Jackson Laboratories. Mice were bred from heterozygous breeding pairs, and littermate control *Aire*$^{+/+}$ mice were used. *Aire*$^{-/-}$ mice were crossed to NOD *Tcrα*$^{-/-}$ mice to generate *Aire*$^{-/-}$*Tcrα*$^{-/-}$ double knockout mice or NOD *Ighm*$^{-/-}$ (μMT) mice to generate *Aire*$^{-/-}$*Ighm*$^{-/-}$ double knockout mice. The mice were used for FACS (BAL, lung), histological/immunohistochemical (lung) and Luminex (BAL) analyses. Mice were age and sex-matched and used when 5-8 weeks-old.

Mouse BAL and lung collection

To collect BAL, mice were sacrificed by anesthetizing the mice with ketamine and xylazine mixture followed by gentle cervical dislocation. The tracheas were exposed, and a small tracheal slit was cut and a BD Insyte Autoguard catheter was placed in the trachea. A syringe was attached to the catheter and 0.75 mL of PBS + 0.1 mM EDTA was infused into the trachea and aspirated back for a total of three infusions. BAL was then centrifuged at 600 x g for 10 minutes at 4°C. The supernatant was collected and stored at -80°C until Luminex analysis. The pelleted cells were washed and processed for FACS.

To collect lung tissue, mice were perfused with PBS. All lung lobes were removed and minced in a collagenase/DNAse solution (3 mg/mL collagenase type IV,

Worthington, #LS004189; 40 U/mL DNAse I, Roche #22067800). The lung pieces were added to the collagenase solution and placed in a water bath for 1 hour at 37°C with shaking. The lung digest was drawn into a syringe through a 20-gauge needle and ejected three times to further dissociate the tissue prior to passage through a 100 µm filter. The cells were washed and residual red blood cells were lysed with ACK lysis buffer. The lung cells were washed, filtered through a 40 µm filter, and used for FACS analysis.

FACS on mouse BAL and lung cells

To analyze cell populations in the mouse lung and BAL, the following fluorochrome-conjugated (BV605, eVolve 605, BV570, eFluor450, FITC, PE, PerCP-Cy5.5, PE-Cy7, APC, AF700, APC-eFluor780 and APC-Cy7) antibodies against mouse antigens were used: CD11b (M1/70) (Biolegend); B220 (RA3-6B2), NKp46 (29A1.4), CD45 (30-F11), CD4 (RM4-5 or GK1.5), CD3 (145-2C11 or 17A2), CD19 (eBio1D3), CD8 (53-6.7) (Thermo Fisher Scientific); Ly6G (1A8) (BD Biosciences). Briefly, dead cells were excluded using the Live/Dead Blue Dead Cell Stain Kit and Fc blockade was performed using rat anti-mouse CD16/32 (Thermo Fisher Scientific). Cell-surface molecules were then stained, cells were resuspended in FACS buffer, data collected on an LSR Fortessa and analyzed using FlowJo software. Cell numbers were quantified using counting PE-conjugated beads (Spherotech) (*57*).

Luminex

To assess the neutrophil-targeted CXC chemokines in human (CXCL1, CXCL2, CXCL8) and mouse (CXCL1, CXCL2) BAL, a Luminex array was performed as previously described (*58*).

Histology

Lungs were harvested at 6-8 weeks of age, fixed in formalin, and embedded in paraffin. Tissue sections were processed for Hematoxylin & Eosin (H&E) staining (Histoserve, Inc.) and immunohistochemical stains CD3 (CD3-12, Bio-Rad cat# MCA1477) and CD45R/B220 (RA3-6B2, BD Biosciences, cat# 553086) (Pathology/Histotechnology Laboratory, Leidos Biomedical Research, Inc.) Sections were viewed under a microscope and scored based on the following system: grade 0, normal lung; grade 1, infrequent peribronchiolar and perivascular infiltrates and interstitial aggregates affecting; grade 2, frequent peribronchiolar and perivascular infiltrates and interstitial aggregates; grade 3, dense and confluent peribronchiolar and perivascular infiltrates and interstitial aggregates affecting; grade 4, diffuse peribronchiolar and perivascular infiltrates and interstitial aggregates with architectural distortion (*4, 5*).

Figure S1

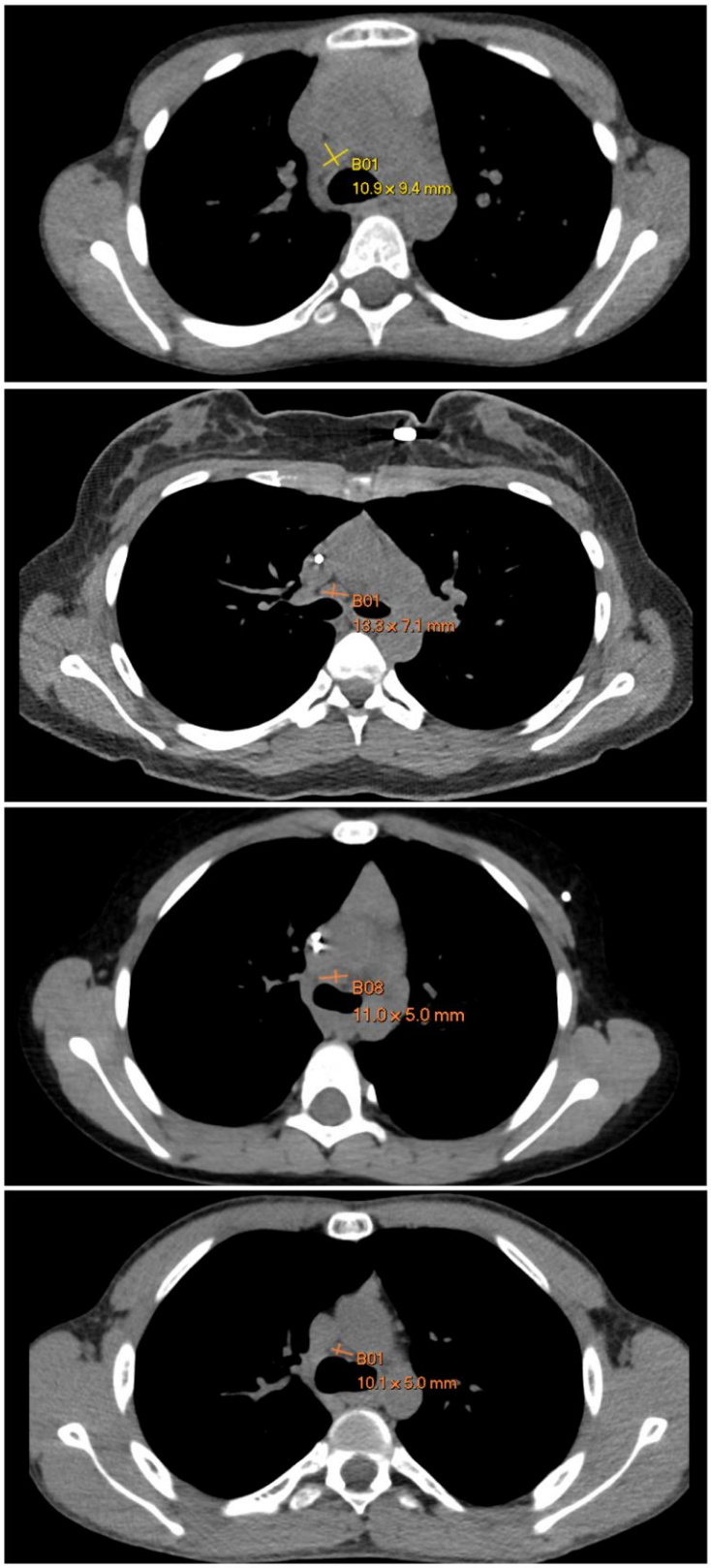

Fig. S1. Enlarged mediastinal lymph nodes in patients with APECED pneumonitis. Shown are images of non-contrast chest CT scans from four APECED patients with autoimmune pneumonitis.

Figure S2

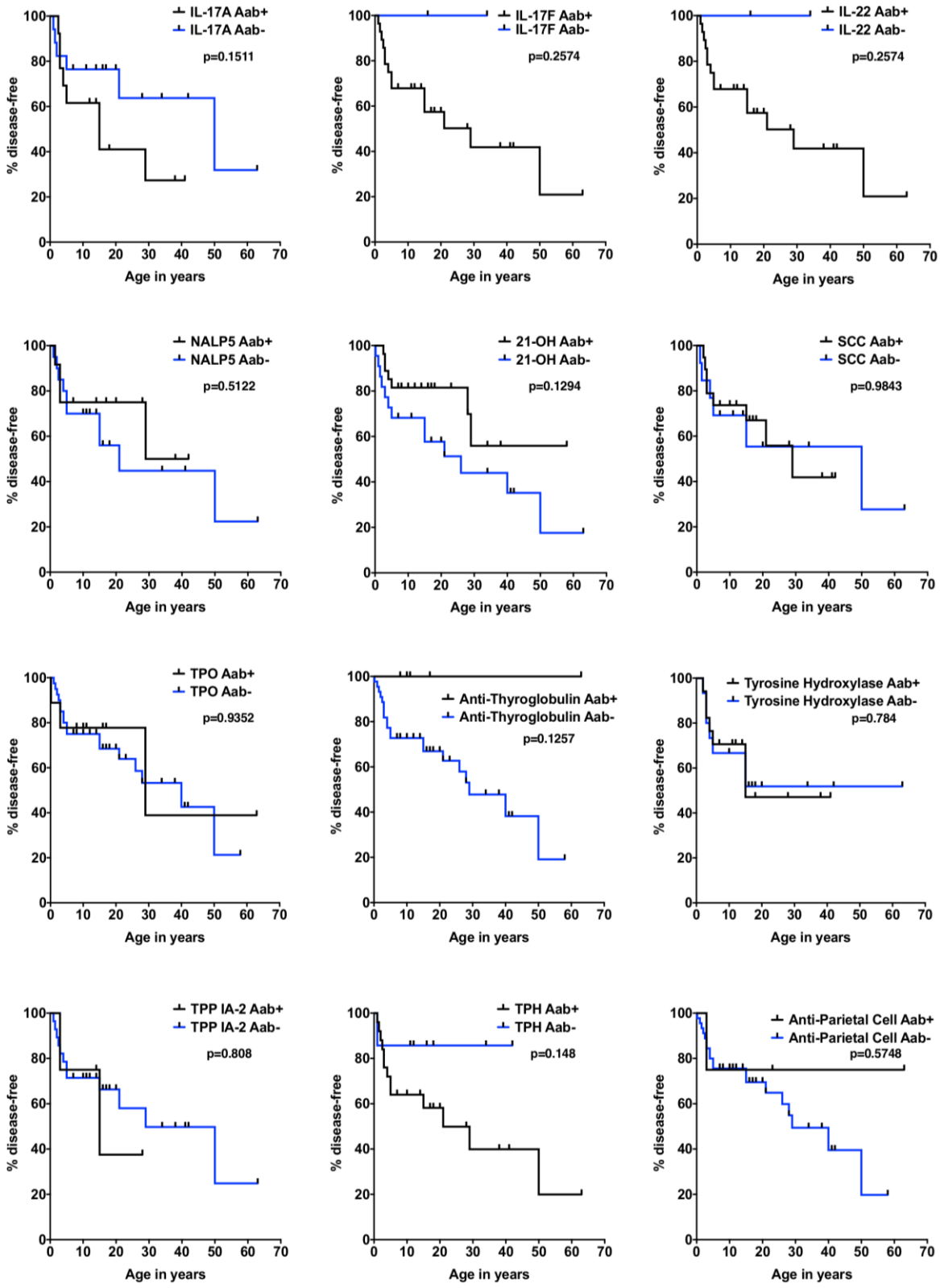

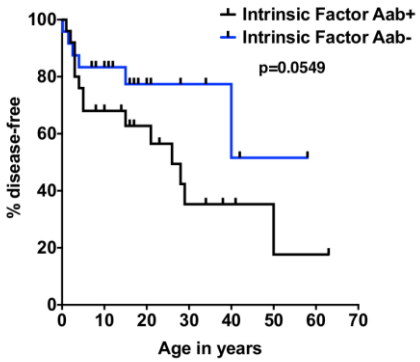

Fig. S2. Association of autoantibody reactivity against cytokines and tissue-specific autoantigens and the time to development of pneumonitis in patients with APECED. Shown are Kaplan-Meier curves illustrating the relationship between the time to development of pneumonitis with the presence or absence of the corresponding autoantibodies (n=30-49). IL-17A, interleukin-17A; IL-17F, interleukin-17F; IL-22, interleukin-22; NALP5, NLR family and pyrin domain containing 5; 21-OH, 21-hydroxylase; SCC, side chain cleavage; TPO, thyroid peroxidase; TPP IA-2, tyrosine phosphate-related islet antigen 2; TPH, tryptophan hydroxylase.

Figure S3

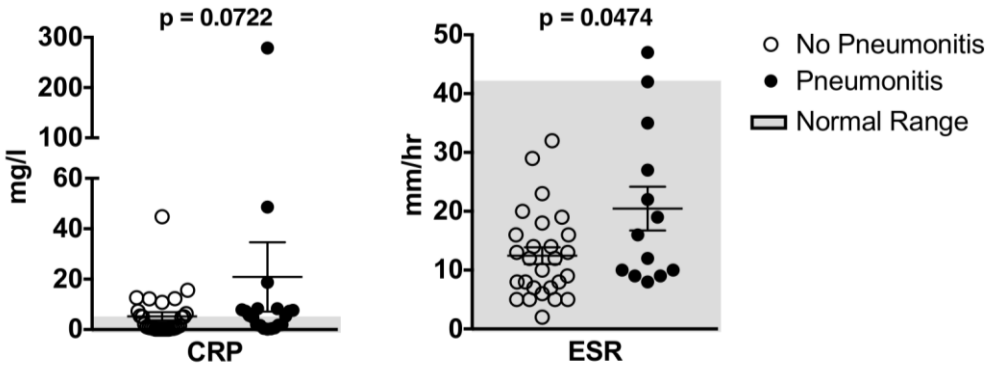

Fig. S3. Serum inflammatory markers in patients with APECED pneumonitis. Shown are concentrations of C-reactive protein (CRP) (n=49) and erythrocyte sedimentation rate (ESR) (n=40) in the sera of APECED patients with or without pneumonitis. The gray shaded areas represent the normal range for the corresponding marker. Patients receiving intravenous immunoglobulin were excluded from the ESR analyses. A Mann-Whitney test was used for statistical analyses. Quantitative data represents mean ± SEM.

Figure S4

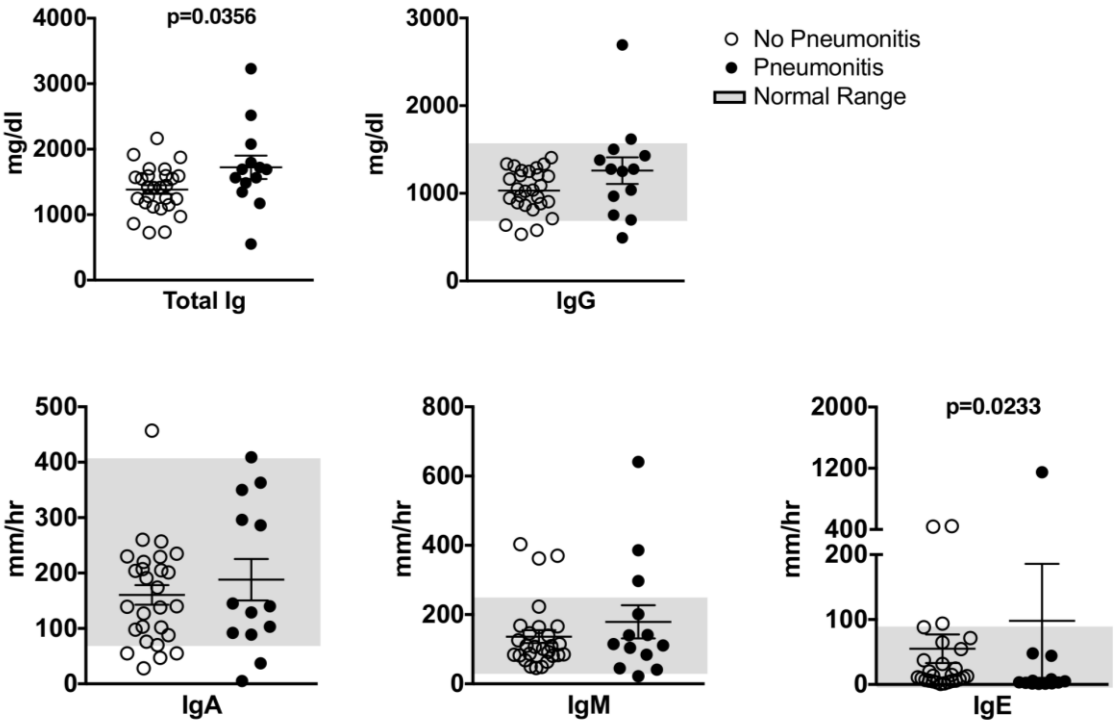

Fig. S4. Immunoglobulin concentrations in patients with APECED pneumonitis. Shown are concentrations of total immunoglobulin (Ig), IgG, IgA, IgM, and IgE in the sera of APECED patients with or without pneumonitis (n = 40). The gray shaded areas represent the normal range for the corresponding immunoglobulin. Patients receiving intravenous immunoglobulin were excluded from the analysis. A Mann-Whitney test was used for statistical analyses. Quantitative data represents mean ± SEM.

Figure S5

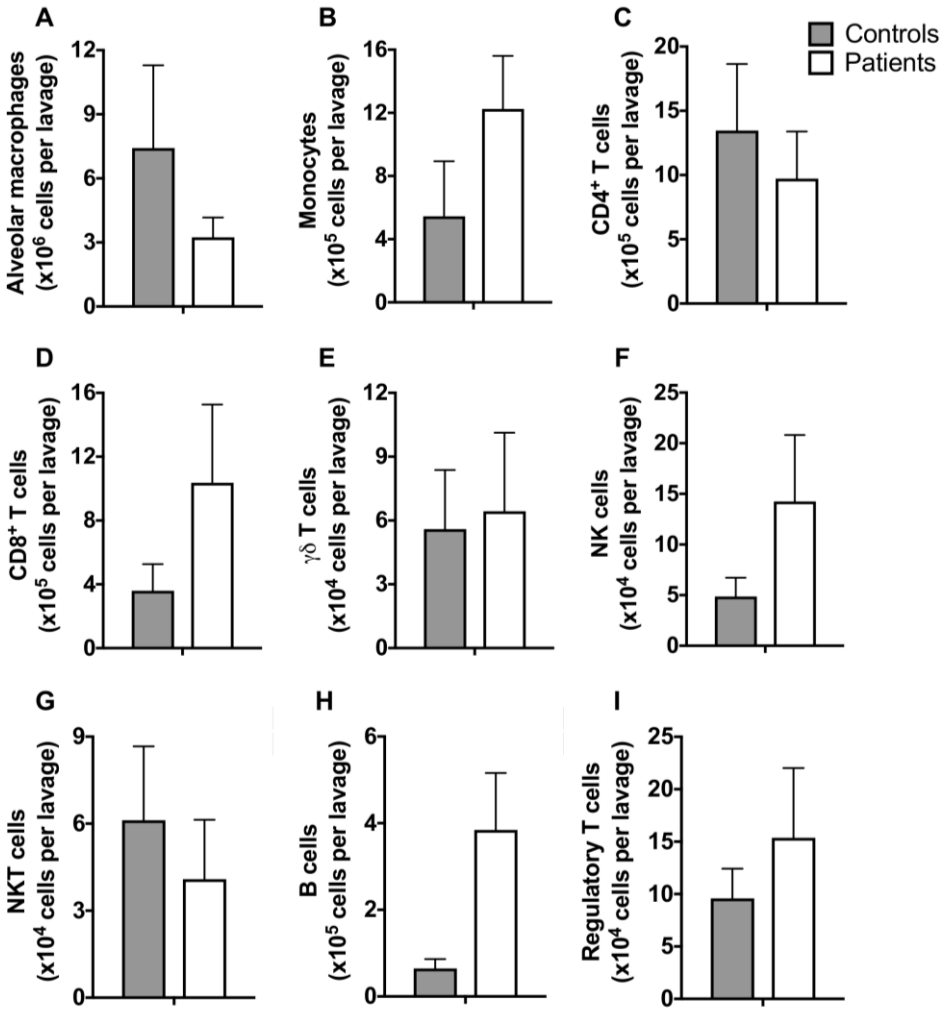

Fig. S5. Leukocyte subsets other than neutrophils do not exhibit increased accumulation in the airways of patients with APECED pneumonitis. Shown are total numbers of alveolar macrophages (**A**), monocytes (**B**), $CD4^+$ T cells (**C**), $CD8^+$ T cells (**D**), γδ T cells (**E**), NK cells (**F**), NKT cells (**G**), B cells (**H**) and regulatory T cells (**I**) in the bronchoalveolar lavage fluid of APECED patients with pneumonitis (n=5) relative to healthy controls (n=4). Data represent mean ± SEM. Differences between groups were determined using unpaired t-test (panels C-E, G, I), unpaired t-test with Welch's correction (panels A, F, H) or Mann-Whitney test (panel B); no statistically significant differences were identified.

Figure S6

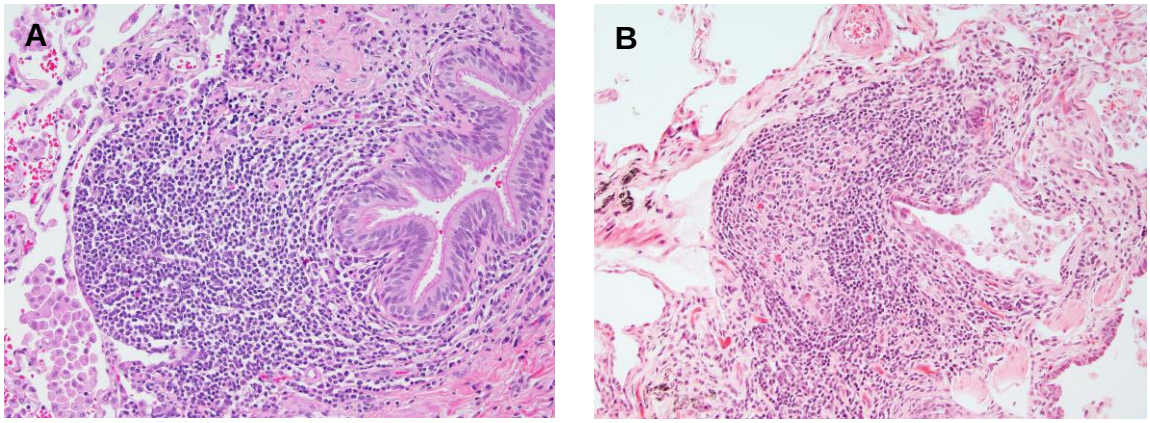

Fig. S6. Primary lymphoid follicle and germinal center formation in lung tissue of patients with APECED pneumonitis. Shown is a primary lymphoid follicle adjacent to a bronchiole (**A**) and a germinal center adjacent to a damaged bronchiole (**B**) observed in lung tissues obtained from two APECED patients. 200x magnification.

Figure S7

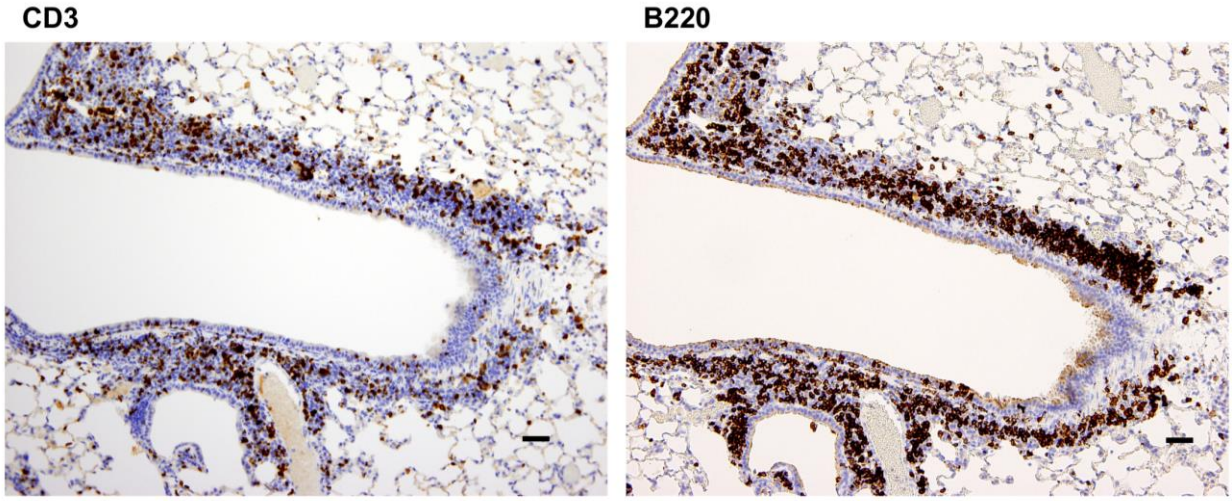

Fig. S7. Intraepithelial lymphocyte infiltration in *Aire*$^{-/-}$ mouse lung tissue. Shown are immunohistochemical stains with lymphocyte markers CD3 and B220 in *Aire*$^{-/-}$ mouse lung. Original magnification, 200x. Scale bars, 80μm.

Figure S8

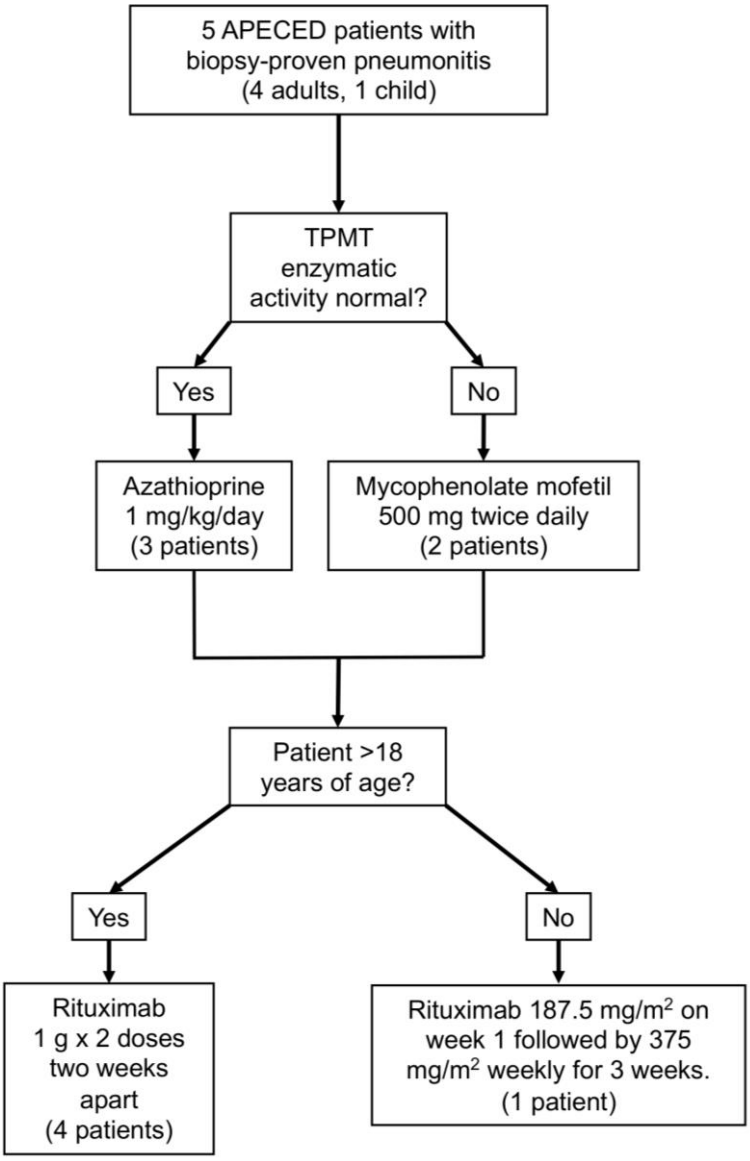

Fig. S8. Schematic illustration of the lymphocyte-directed immunomodulation used in this study. Shown is a schematic for the selection of the T lymphocyte-modulating agent (azathioprine or mycophenolate mofetil) based on the results of the thiopurine methyltransferase (TPMT) enzymatic activity. The dosing of rituximab was determined by the patient age and weight.

Figure S9

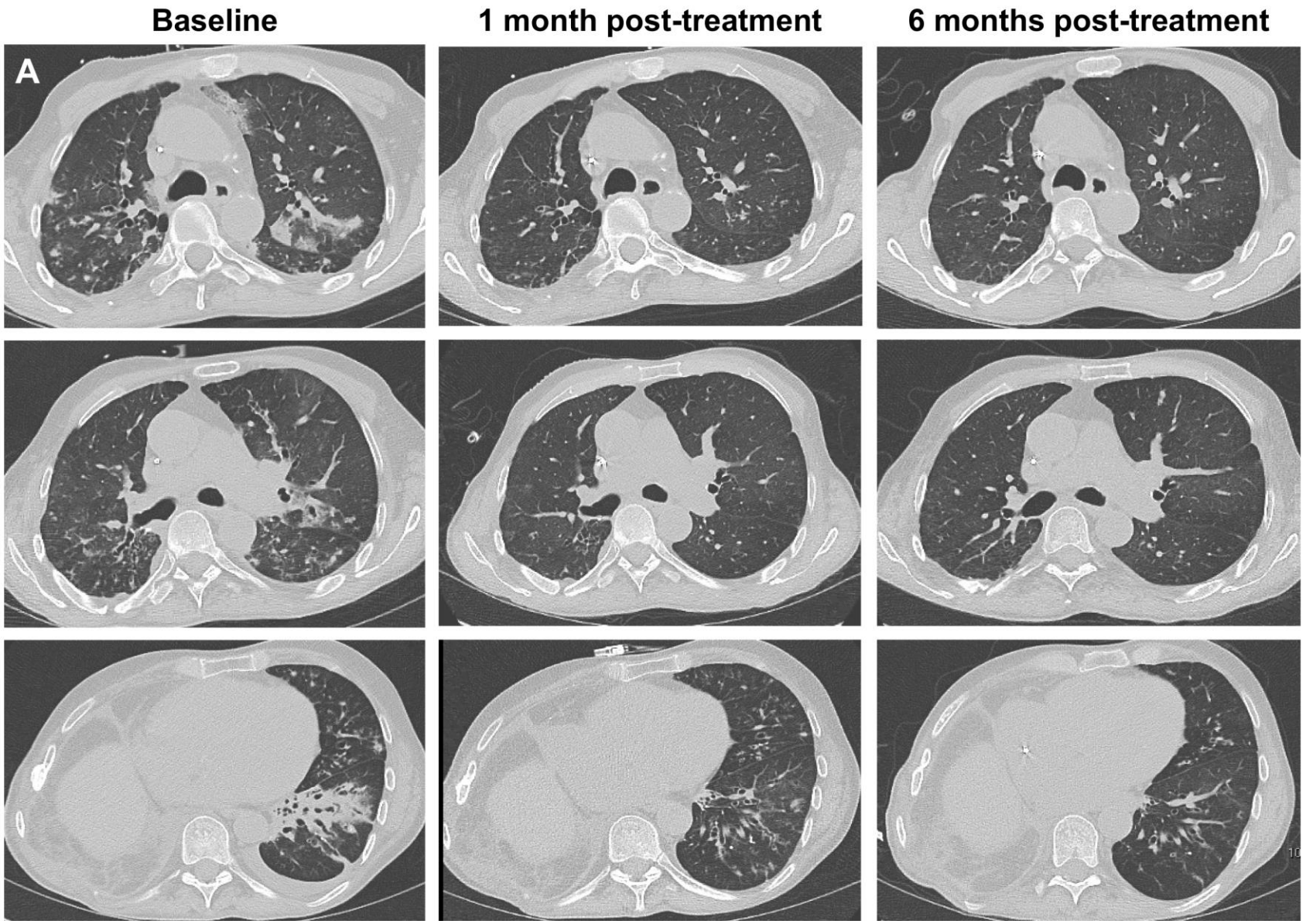

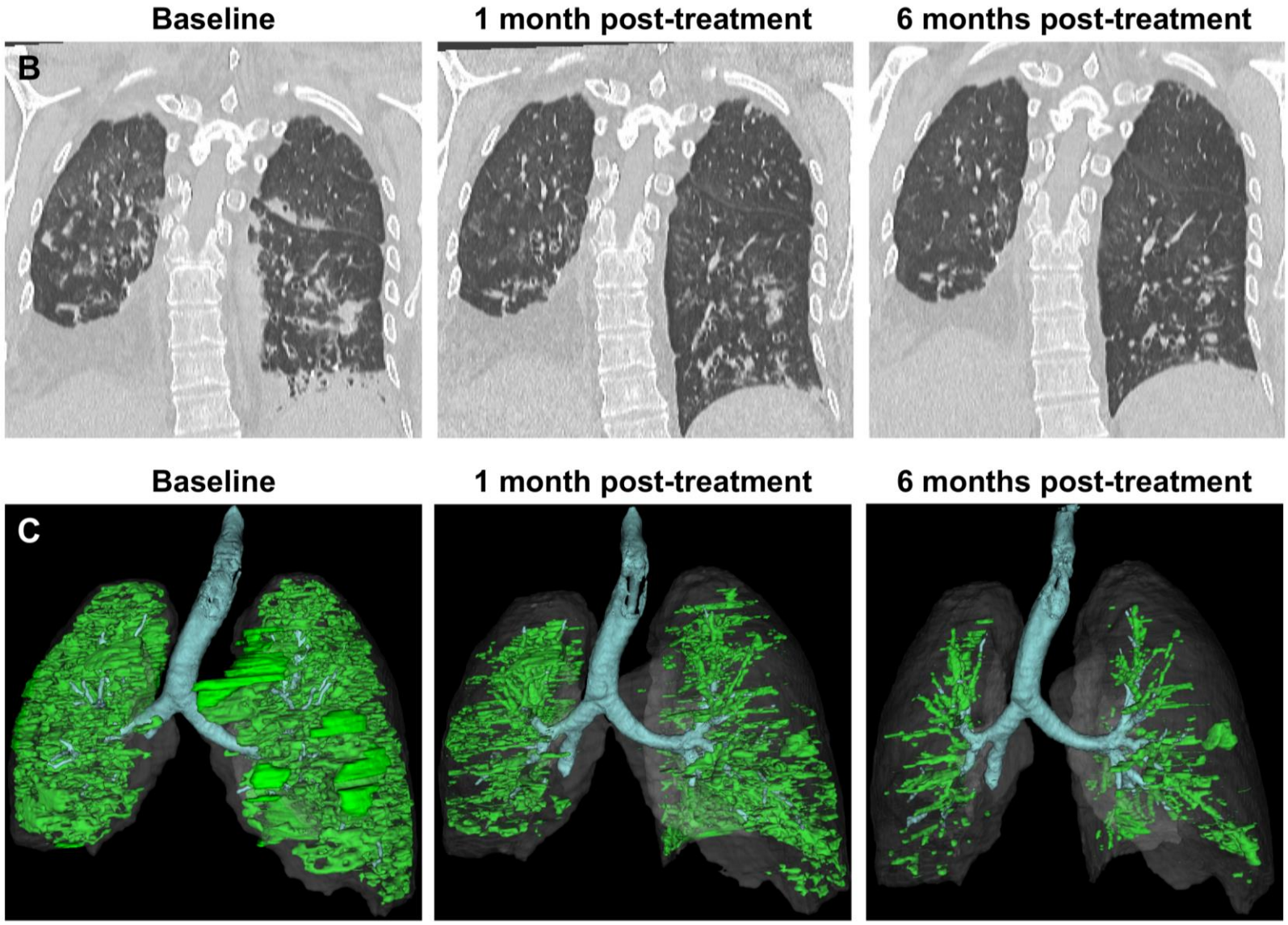

Fig. S9. Treatment response assessed by radiography in patient 1. Shown are serial axial (**A**) and coronal (**B**) chest CT images and coronal 3D reconstructed CT images (**C**) at baseline and at 1 and 6 months after treatment initiation.

Figure S10

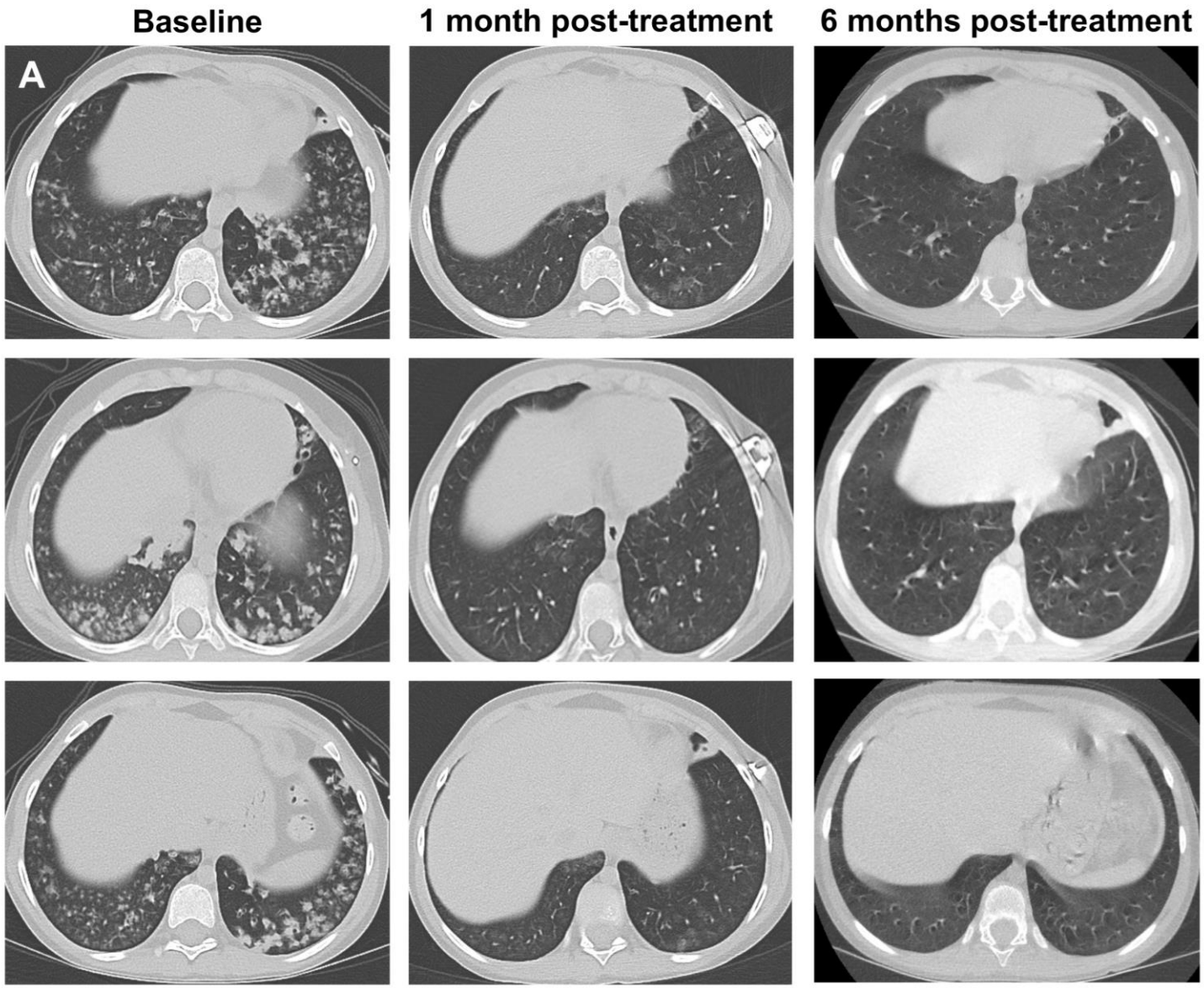

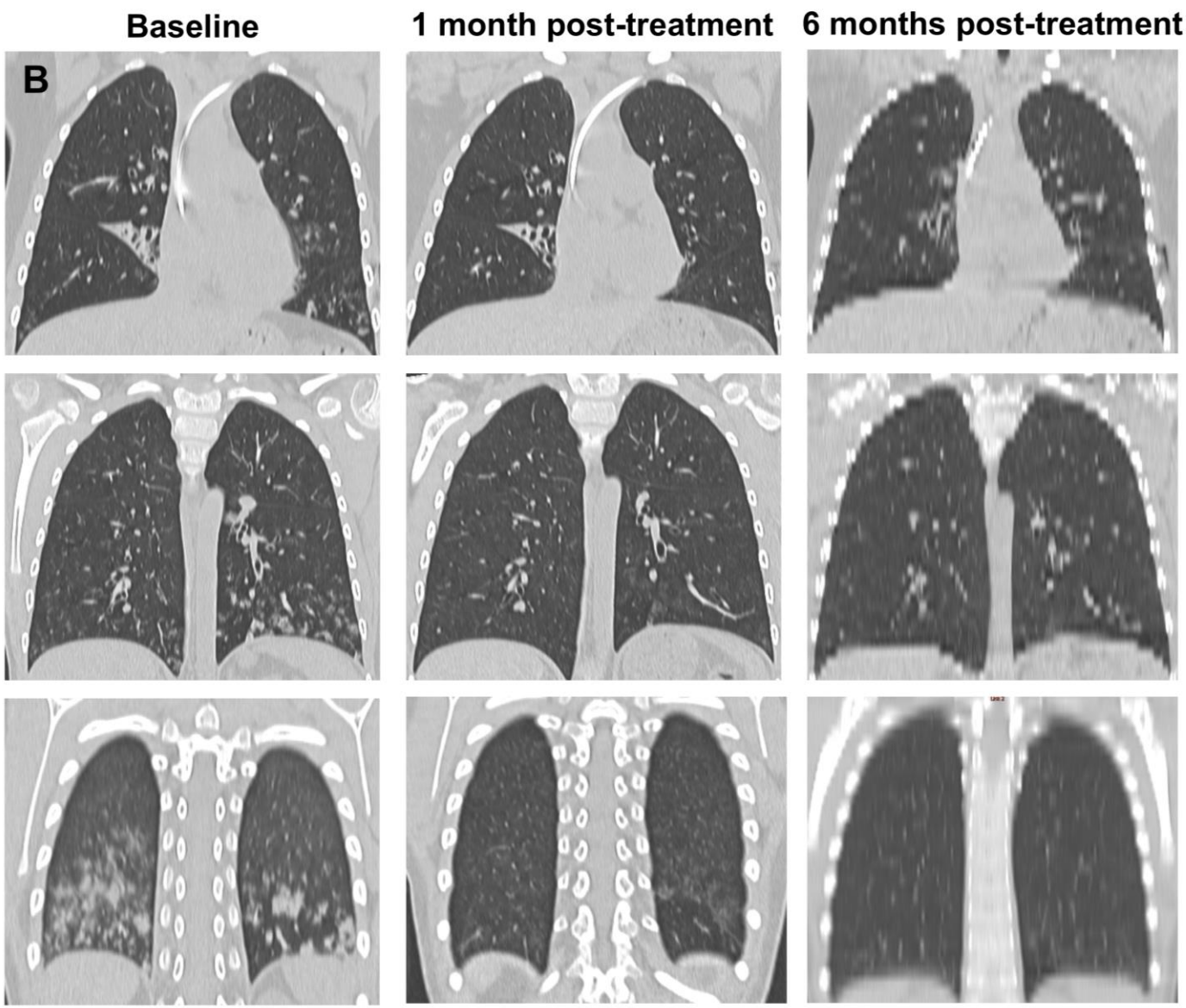
Baseline
1 month post-treatment
6 months post-treatment
B

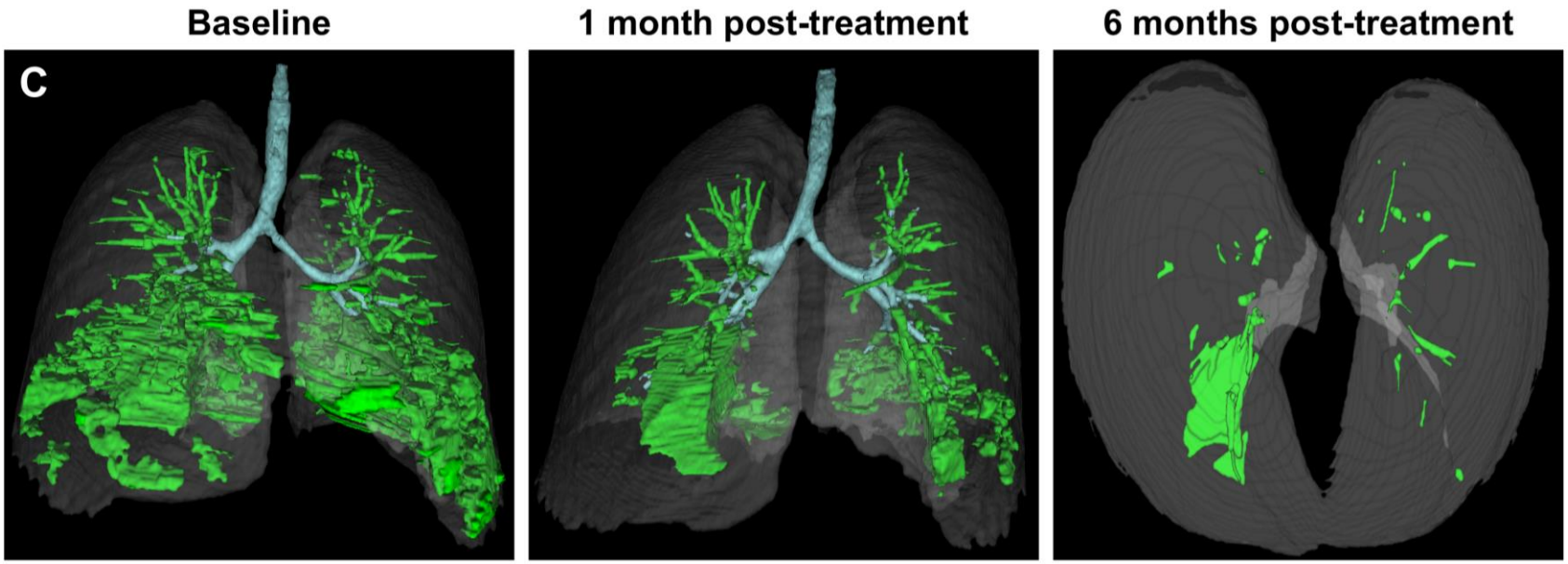

Fig. S10. Treatment response assessed by radiography in patient 2. Shown are serial axial (**A**) and coronal (**B**) chest CT images and coronal 3D reconstructed CT images (**C**) at baseline and at 1 and 6 months after treatment initiation.

Figure S11

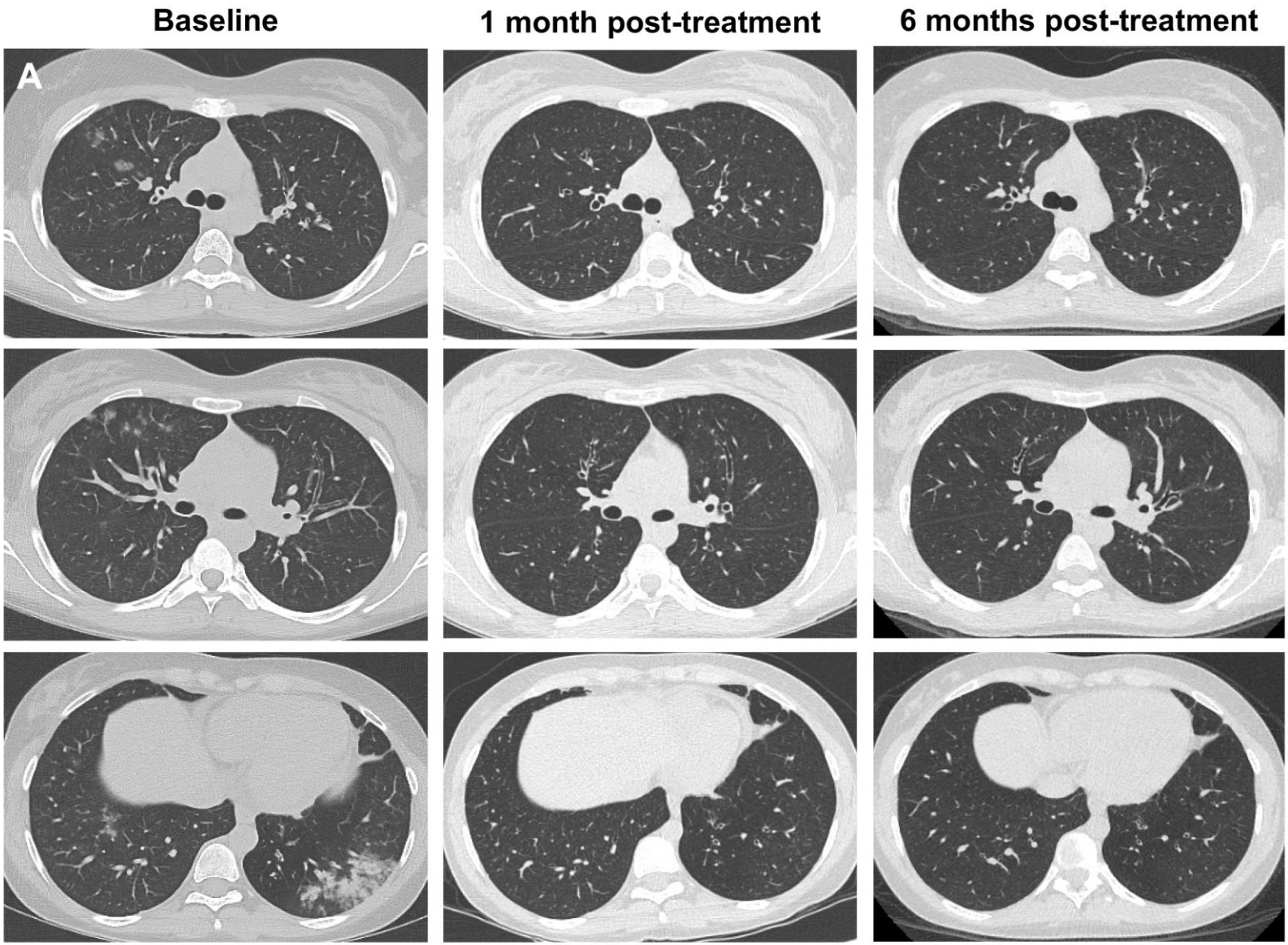

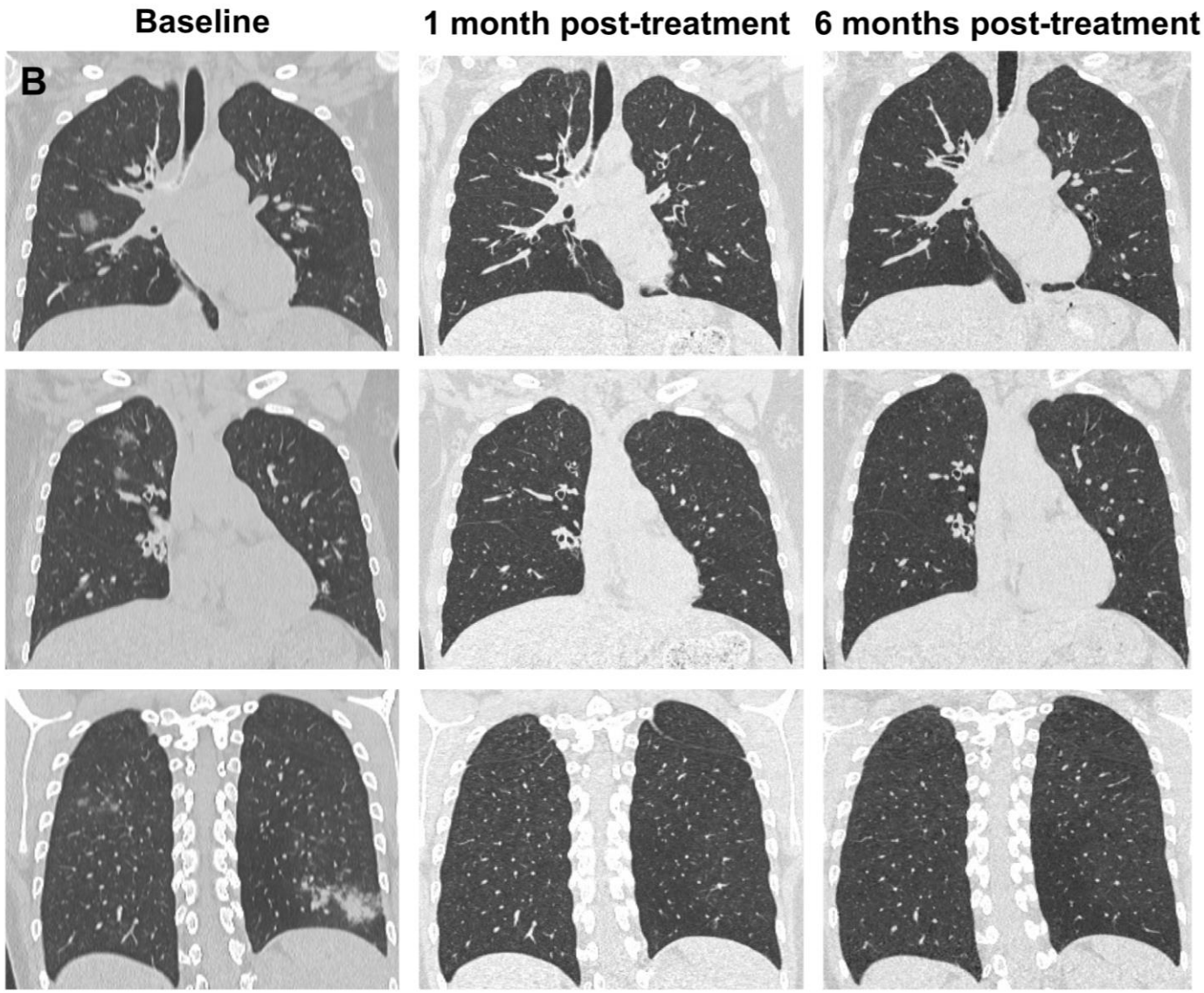
Baseline
1 month post-treatment
6 months post-treatment
B

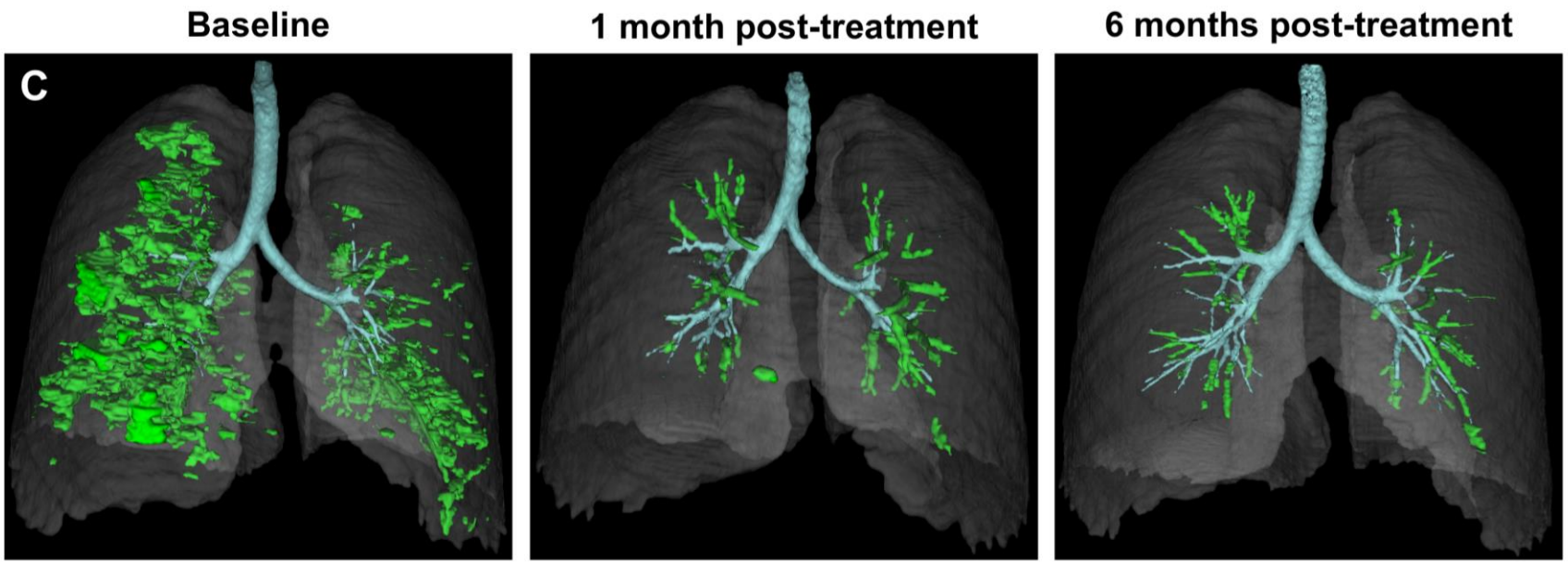

Fig. S11. Treatment response assessed by radiography in patient 3. Shown are serial axial (**A**) and coronal (**B**) chest CT images and coronal 3D reconstructed CT images (**C**) at baseline and at 1 and 6 months after treatment initiation.

Figure S12

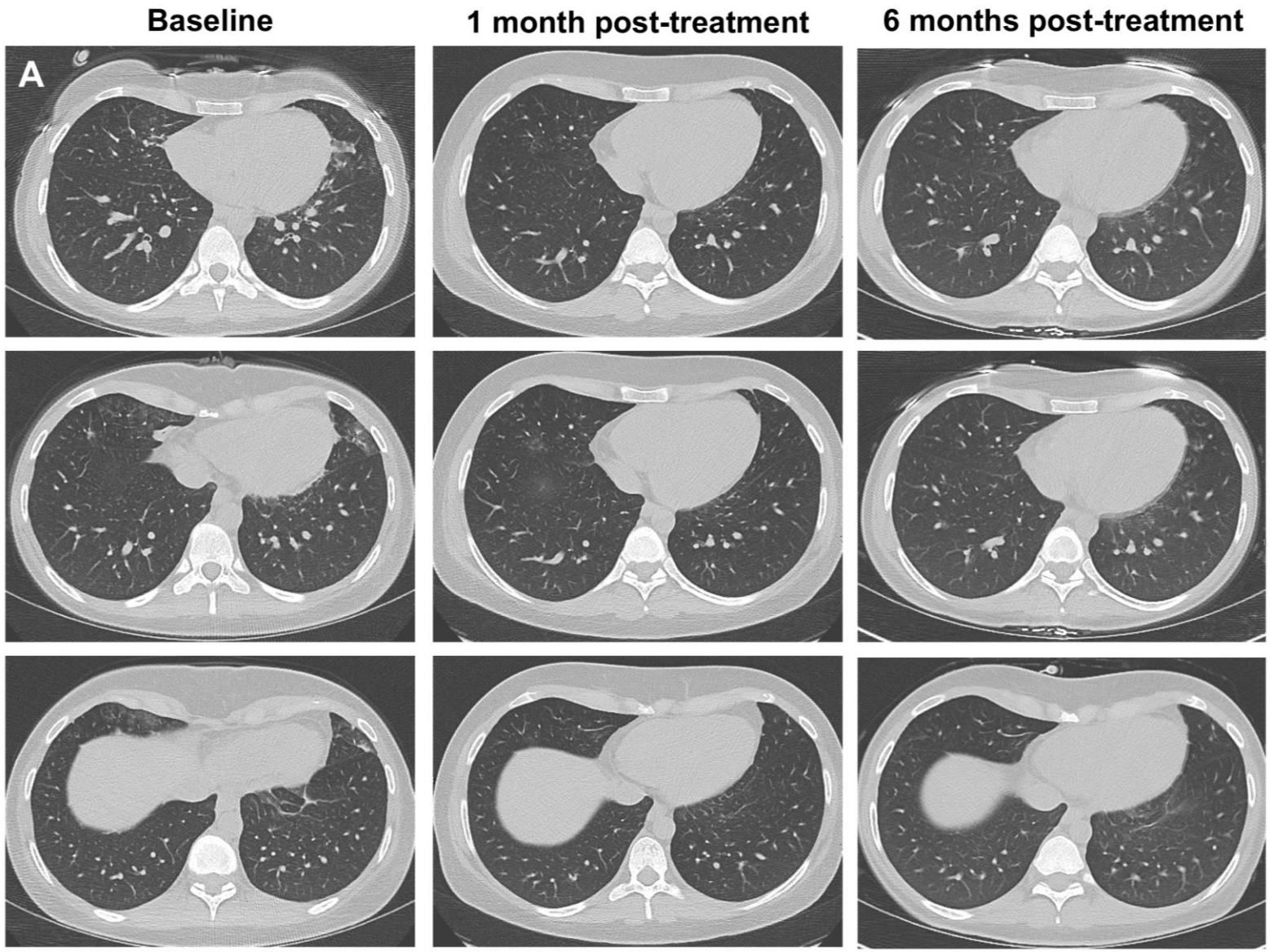

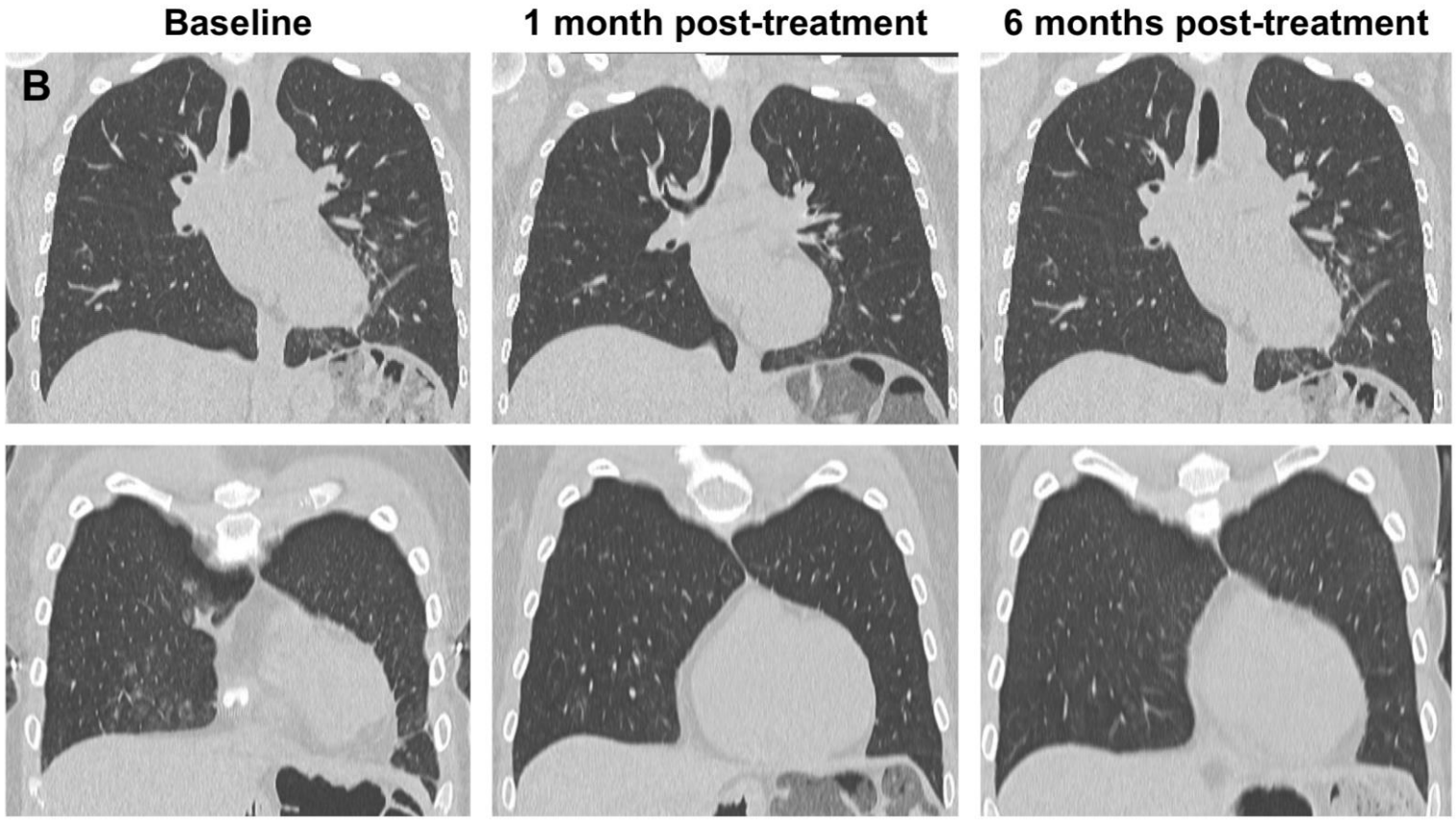
Baseline
1 month post-treatment
6 months post-treatment
B

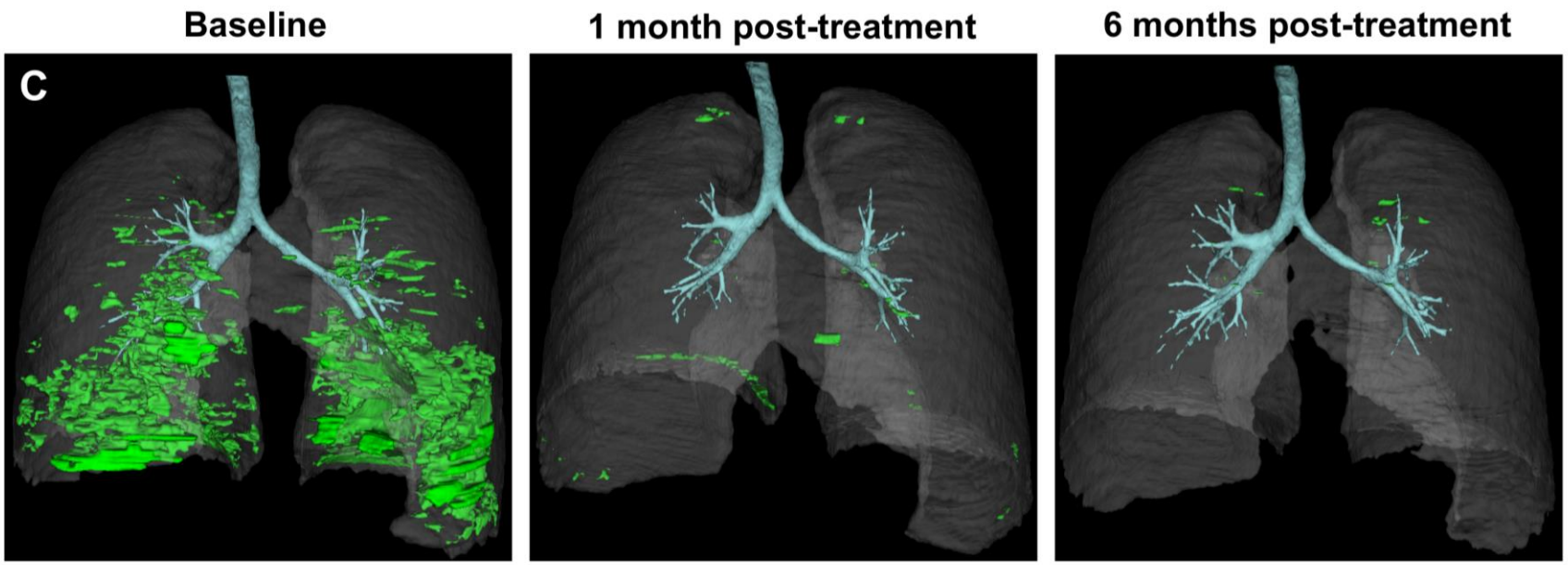

Fig. S12. Treatment response assessed by radiography in patient 4. Shown are serial axial (**A**) and coronal (**B**) chest CT images and coronal 3D reconstructed CT images (**C**) at baseline and at 1 and 6 months after treatment initiation.

Figure S13

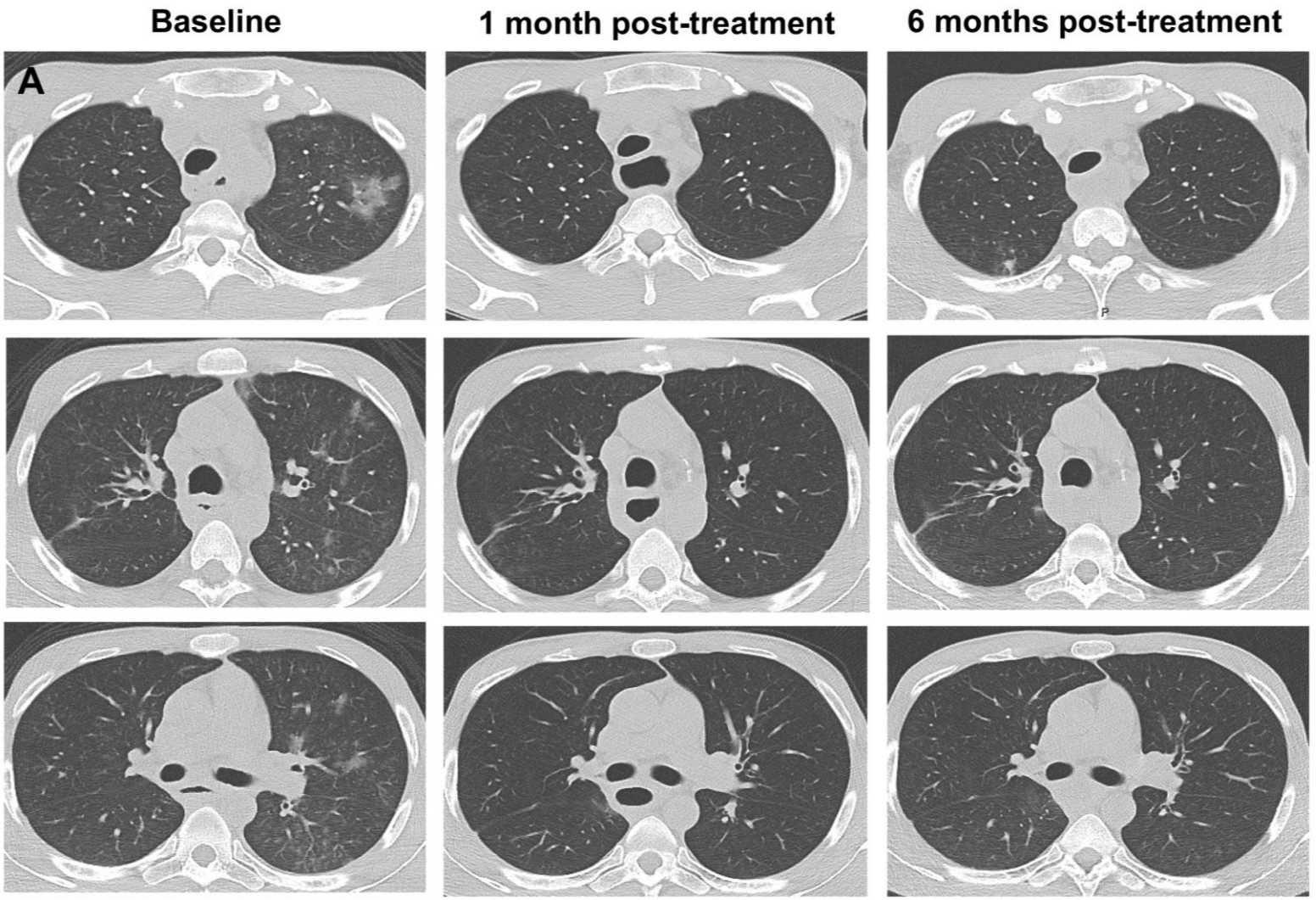

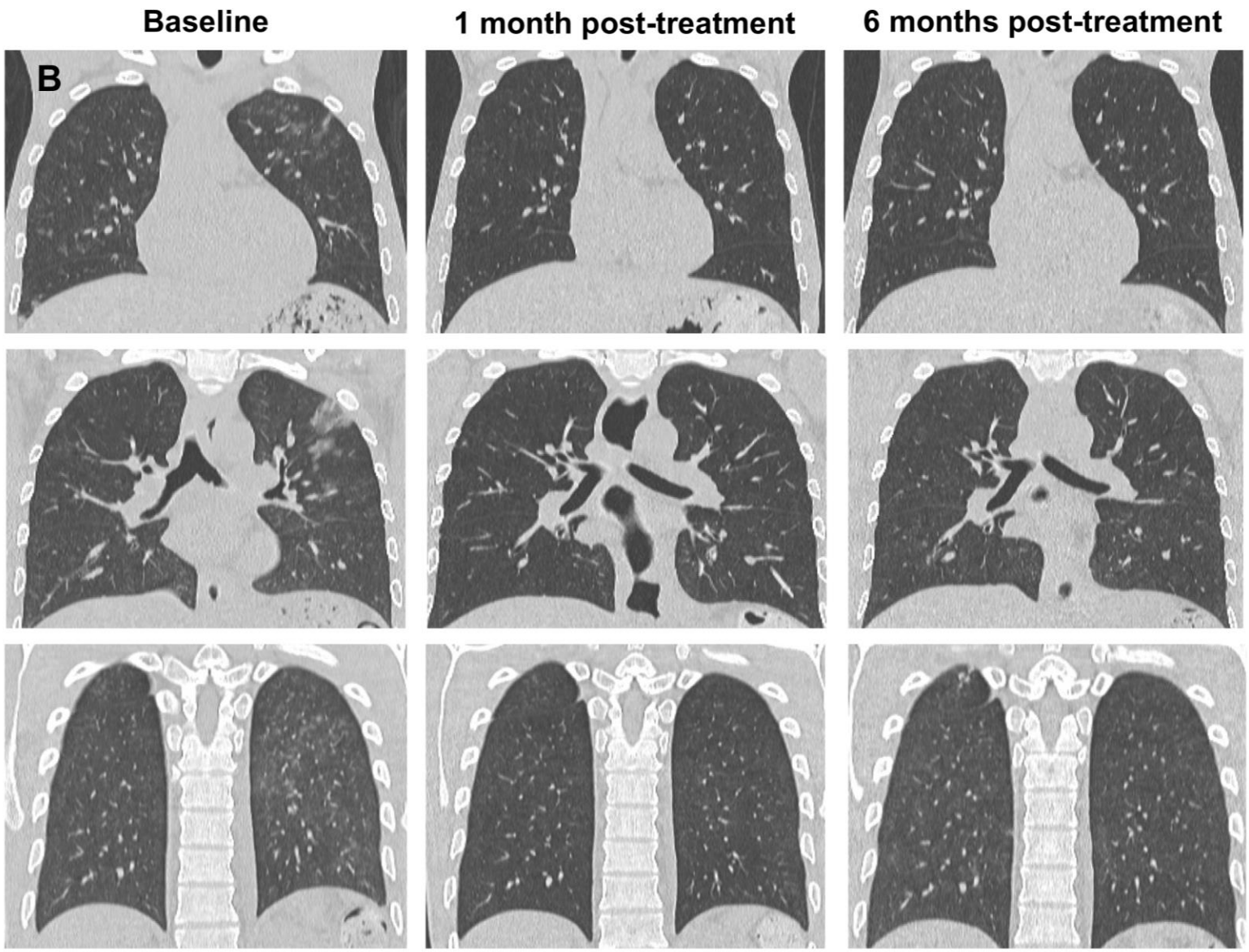
Baseline
1 month post-treatment
6 months post-treatment
B

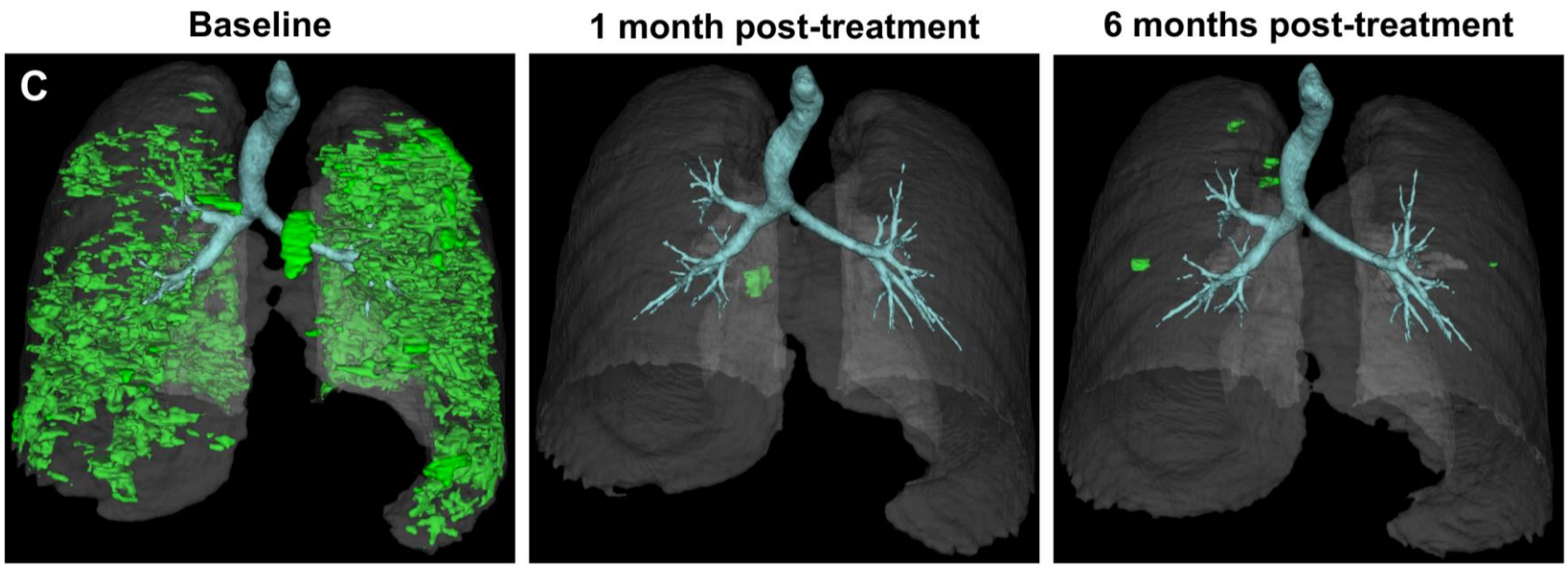

Fig. S13. Treatment response assessed by radiography in patient 5. Shown are serial axial (**A**) and coronal (**B**) chest CT images and coronal 3D reconstructed CT images (**C**) at baseline and at 1 and 6 months after treatment initiation.

Figure S14

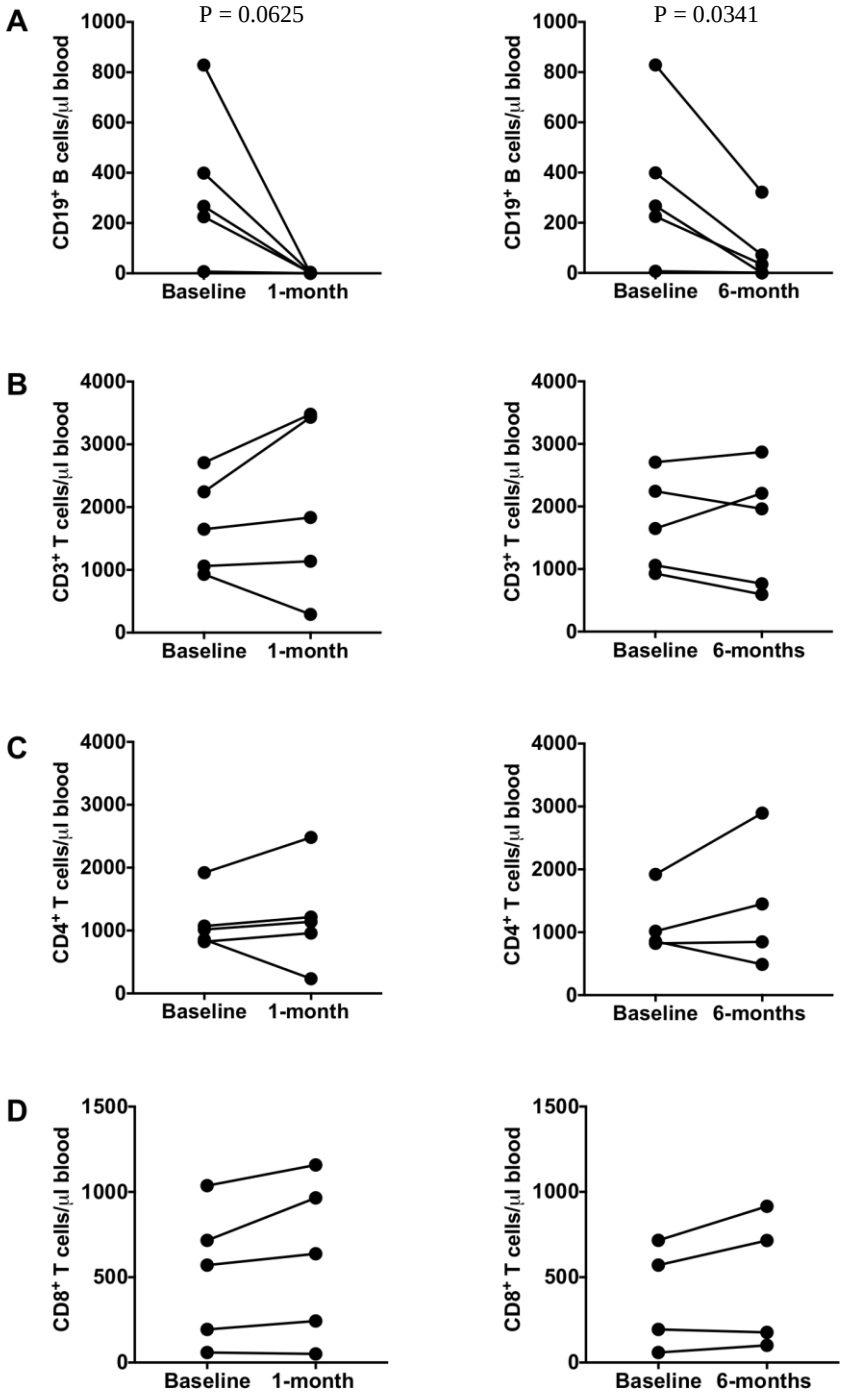

Fig. S14. Lymphocyte-directed immunomodulation causes rapid depletion of B, but not T, lymphocytes in peripheral blood of patients with APECED with pneumonitis. Comparison of $CD19^+$ B lymphocytes (**A**, n=5), $CD3^+$ T lymphocytes (**B**, n=5), $CD4^+$ T lymphocytes (**C**, n=4-5), and $CD8^+$ T lymphocytes (**D**, n=4-5), at baseline versus at 1 and 6 months after treatment initiation. The lymphocyte phenotyping panel of Patient 2 (table S1) was performed at an outside facility that did not include $CD4^+$ and $CD8^+$ T lymphocyte subpopulations. Differences between $CD4^+$ T lymphocytes at baseline and 1

or 6 months, between $CD8^+$ T lymphocytes at baseline and 6 months and between $CD19^+$ B cells at baseline and 1 month were determined using the Wilcoxon test. Differences between $CD3^+$ T lymphocytes at baseline and 1 or 6 months, between $CD8^+$ T lymphocytes at baseline and 1 month and between $CD19^+$ B cells at baseline and 6 months were determined using a paired t-test.

Figure S15

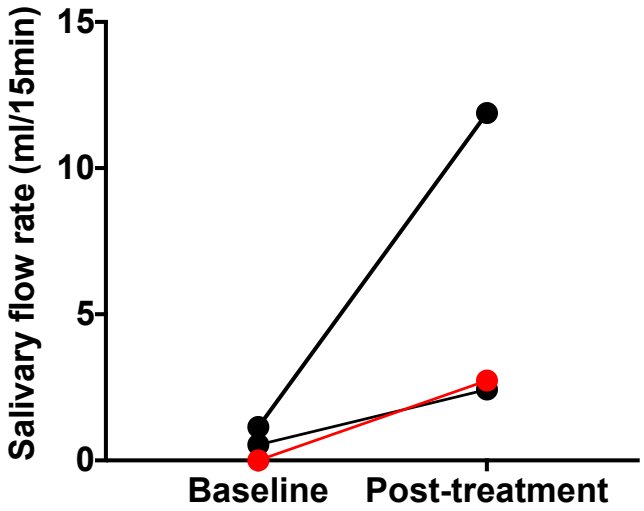

Fig. S15. Lymphocyte-directed immunomodulation improves salivary production in patients with APECED with Sjogren's-like syndrome. Shown are salivary flow rates obtained at baseline and within 6 (n=2; black dots) to 12 months (n=1; red dots) from treatment initiation.

Figure S16

Fig. S16. Lymphocyte-directed immunomodulation caused resolution of nail dystrophy in one of the three patients with APECED with this condition.
Photographs depict dystrophic nails before treatment and normal nail growth 6 months after treatment initiation.

Table S1. Demographic and geographic origin characteristics of our patients with APECED.

	Pneumonitis (n=21)	Non-pneumonitis (n=29)	All patients (n=50)
Mean age (range)	27.6 (9 to 56)	24.3 (8 to 66)	25.7 (8 to 66)
Number of pediatric patients (%)	6 (28.6)	12 (41.4)	18 (36)
Number of males (%)	5 (23.8)	15 (51.7)	20 (40)
Number of females (%)	16 (76.2)	14 (48.3)	30 (60)
Number of Caucasian patients (%)	17 (81)	28 (96.5)	45 (90)
Number of Hispanic patients (%)	4 (19)	1 (3.5)	5 (10)
Residence outside of the US	3 (13.6)	4 (13.8)	7 (14)
Australia	1	0	
Argentina	1	0	
Canada	1	0	
Colombia	0	1	
Germany	0	1	
Isle of Man (UK)	0	1	
United Arab Emirates	0	1	
Residence in the US	18 (85.7)	25 (56.8)	43 (86.0)
California	0	1	
Colorado	1	2	
Connecticut	2	0	
Florida	2	0	
Georgia	2	0	
Indiana	0	1	
Louisiana	1	0	
Maryland	0	2	
Michigan	1	0	
Minnesota	0	1	
Mississippi	0	1	
Missouri	1	1	
New Jersey	1	1	
New York	1	5	
North Carolina	2	0	
Ohio	0	3	
Oregon	0	1	
Pennsylvania	1	0	
Tennessee	1	0	
Texas	1	1	
Virginia	1	3	
Wisconsin	0	3	

Table S2. Demographic, clinical, and radiographic response characteristics of the five patients with APECED pneumonitis who received lymphocyte-directed immunomodulation.

Patient*	Age in years	Gender	Duration of pneumonitis symptoms before diagnosis (years)	T cell therapy	Other APECED manifestations	Radiography score			% Residual radiographic abnormalities based on CT scoring (based on lesion volume in Hounsfield units)		
						Baseline	1 month	6 months	Baseline	1 month	6 months
1 (#1)	52	M	47	Azathioprine	CMC, SS, ID, G, HP, EH, AI, B12, HTN, V, HG	25	11	11	100	44 (28.618)	44 (6.833)
2 (#9)	7	F	6	Mycophenolate	UE, CMC, ID, HP, AIH, G, EH, ND, AL, GHD, SS,	24	6	4	100	25 (22.903)	16.7 (6.112)
3 (#15)	19	F	16	Azathioprine**	CMC, ID, HP, HT, AIH, UE, AI, KC, ND, EH	17	3	2	100	17.6 (10.987)	11.8 (6.356)
4 (#16)	26	F	22	Azathioprine**	CMC, ID, AIH, AI, HP, UE, AL, EH, Asp, HG, SS	9	0	0	100	0 (2.106)	0 (0.356)
5 (#20)	28	M	n/e	Mycophenolate	CMC, ID, B12, HT, AI, AL,	5	0	1	100	0 (0.275)	20 (0.292)

					SS, ND, Asp						
									Mean	17.32 (12.978)	18.5 (3.9898)

M, male; F, female; CMC, chronic mucocutaneous candidiasis; HP, hypoparathyroidism; AI, adrenal insufficiency; HT, hypothyroidism; HG, hypogonadism; GHD, growth hormone deficiency; ID, intestinal dysfunction; G, gastritis; B12, B12 deficiency; AIH, autoimmune hepatitis; Asp, asplenia; SS, Sjogren's-like syndrome; EH, enamel hypoplasia; UE, urticarial eruption; AL, alopecia; V, vitiligo; ND, nail dystrophy; KC, keratoconjunctivitis; n/e, not evaluable. *Patient numbers in parentheses refer to the patient numbers in tables S3 and S6. **Azathioprine was initiated before for treatment of autoimmune hepatitis in these two patients.

Table S3. Patients with APECED pneumonitis do not carry serum autoantibodies against MDA5.

Patient #	MDA5 autoantibody immunoreactivity (LU)
1	1149
2	1074.5
3	1526
4	1246
5	1360
6	1623.5
7	1417.5
8	1852
9	1172
10	1189
11	1228.5
12	1155
13	1212
14	1394.5
15	1337.5
16	1383
17	1275
18	1183.5
19	1303
20	1406
21	1326

Shown is autoantibody immunoreactivity against melanoma differentiation-associated protein 5 (MDA5) as light units (LU) using LIPS immunoassay in the 21 APECED patients with pneumonitis. As positive control, LU values of MDA5 autoantibody positivity in patients with polymyositis/dermatomyositis range from 131,163.5 to 613,736.5 (n=3).

Table S4. Percent of lymphocyte subsets within corresponding lymphocytes in the peripheral blood of patients with APECED with or without pneumonitis.

	Pneumonitis patients (n=20)		Non-pneumonitis patients (n=29)		
	% within total lymphocytes				
Cell Subset	Mean (Median)	Range	Mean (Median)	Range	p-value
CD3+ T cells	80.1 (83.6)	28.3-97.6	84.2 (85.8)	67.5-92.8	0.5351
CD4+ T cells	53.7 (54.7)	19.7-76.5	55.6 (53.9)	36.7-84.7	0.5742*
CD4+CD45RA+CD62L+ naïve T cells	26.2 (24.8)	1.5-43.6	29.2 (29.7)	12.1-49.5	0.2518*
CD4+CD45RA-CD62L+ central memory T cells	21.3 (21.5)	6.4-38.3	20.2 (17.6)	10.3-38.5	0.6484*
CD4+CD45RA-CD62L- effector memory T cells	5.8 (5.5)	2-11.2	5.4 (5.0)	1.6-12.1	0.6471*
CD4+CD45RA+CD62L- effector T cells	0.4 (0.1)	0-3	0.2 (0.1)	0-1.8	0.3221
CD8+ T cells	22.7 (23.5)	3.8-33.4	23.6 (22.6)	12.1-42.8	0.8364*
CD8+CD45RA+CD62L+ naïve T cells	12.1 (11.4)	1-25	14.2 (13.9)	1.2-34.7	0.2925*
CD8+CD45RA-CD62L+ central memory T cells	2.7 (2.7)	0.1-5.5	3.2 (3.3)	1.2-9.4	0.3547
CD8+CD45RA-CD62L- effector memory T cells	3.7 (3.2)	0.6-17.3	3.9 (3.2)	0.9-9.6	0.3095
CD8+CD45RA+CD62L- effector T cells	4.2 (1.6)	0.4-16.8	2.3 (1.7)	0.5-8.6	0.8599
CD3+CD4-CD8- double-negative T cells	4.0 (3.3)	0.6-12.9	4.8 (4.0)	1-16.9	0.186
CD20+ B cells	11.4 (12.7)	0.4-30.4	8.6 (6.9)	1-26.8	0.2123*
CD19+ B cells	11.5 (12.7)	0.4-30.4	8.6 (6.9)	1-26.8	0.2014*
CD20+CD27+ memory B cells	1.4 (1.1)	0-3.9	1.8 (1.5)	0.1-4.5	0.2559*
CD20+CD38+ transitional B cells	8.0 (7.5)	0.4-18.2	7.5 (6.9)	0.6-25.1	0.8837
CD20+CD10+ immature B cells	2.0 (1.0)	0-9.5	2.2 (1.6)	0.2-6.3	0.3581
CD21+CD10+ immature B cells	1.3 (0.5)	0-3.6	1.3 (0.5)	0.1-6.2	0.7076
CD20+IgM-CD38high plasmablasts	0.07 (0)	0-0.5	0.03 (0)	0-0.1	0.2217
CD20+IgM+CD10+ immature B cells	2.5 (1.1)	0-10.4	1.9 (1.3)	0.1-6.6	0.858
CD20+CD38+CD10+ early transitional naïve B cells	2.6 (1.2)	0-10.9	2 (1.3)	0.5-5.9	0.8157
CD20+CD27+IgM+ memory non-switched B cells	0.6 (0.5)	0-2.1	0.7 (0.7)	0-2.5	0.5367*
CD20+CD27+IgM- memory switched B cells	0.5 (0.4)	0-1.3	0.7 (0.6)	0-1.9	0.3744
CD3- CD56+ NK cells	8.7 (6.5)	0.6-48.5	7.2 (6.3)	1.4-16.7	0.6036
CD3+ CD56+ NKT cells	6.5 (4.1)	2.1-19.3	7.2 (6.3)	1.1-20.7	0.046

*indicates use of an unpaired t-test. All other comparison data were analyzed by Mann Whitney test.

Table S5. Absolute numbers of lymphocyte subsets in the peripheral blood of patients with APECED with or without pneumonitis.

	Pneumonitis patients (n=20)		Non-pneumonitis patients (n=29)		
	Number of cells per µL of blood				
Cell Subset	Mean (Median)	Range	Mean (Median)	Range	p-value
CD3+ T cells	1654 (1579)	393-2741	2039 (2032)	788-4822	0.0884*
CD4+ T cells	1095 (990)	274-1932	1323 (1257)	602-3387	0.1376*
CD4+CD45RA+CD62L+ naïve T cells	540.6 (552.5)	21-1230	710 (744)	138-1688	0.063*
CD4+CD45RA-CD62L+ central memory T cells	430 (363)	89-1112	469 (407)	203-1063	0.4738
CD4+CD45RA-CD62L- effector memory T cells	114 (94)	35-252	128 (99)	38-532	0.6177
CD4+CD45RA+CD62L- effector T cells	9.8 (2)	0-120	7.4 (3)	0-99	0.0733
CD8+ T cells	467 (450)	59-1037	592 (501)	139-1280	0.1525*
CD8+CD45RA+CD62L+ naïve T cells	232 (229)	13-434	362 (301)	29-1038	0.0347*
CD8+CD45RA-CD62L+ central memory T cells	59 (46)	1-167	75 (69)	18-148	0.1927*
CD8+CD45RA-CD62L- effector memory T cells	87 (47)	8-554	97 (68)	13-310	0.1241
CD8+CD45RA+CD62L- effector T cells	90 (38)	5-450	58 (39)	10-273	0.7129
CD4/CD8 ratio	3.16 (2.26)	1.03-14.43	2.67 (2.16)	1.02-5.79	0.7663
CD3+CD4-CD8- double-negative T cells	85.7 (62)	7-299	115 (105)	28-277	0.0724
CD20+ B cells	286 (246)	9-1216	221 (133)	15-809	0.9784
CD19+ B cells	289 (246)	9-1216	221 (133)	15-809	0.9611
CD20+CD27+ memory B cells	31 (26)	0-77	49 (30)	2-247	0.3043
CD20+CD38+ transitional B cells	203 (129)	9-672	192 (119)	9-757	0.7329
CD20+CD10+ immature B cells	51.7 (18.5)	0-304	55 (44)	3-226	0.2696
CD21+CD10+ immature B cells	37 (10)	0-256	32 (14)	1-187	0.4838
CD20+IgM-CD38high plasmablasts	1 (0)	0-7	0.8 (0)	0-5	0.2946
CD20+IgM+CD10+ immature B cells	63 (25)	0-291	46 (36)	1-199	0.54
CD20+CD38+CD10+ early transitional naïve B cells	65 (28)	0-294	49 (36)	1-211	0.5258
CD20+CD27+IgM+ memory non-switched B cells	15 (11)	0-41	21 (13)	0-137	0.6527
CD20+CD27+IgM- memory switched B cells	13 (8)	0-52	18 (11)	0-49	0.2241
CD3- CD56+ NK cells	153 (143)	11-674	163 (140)	27-274	0.3936
CD3+ CD56+ NKT cells	133 (106)	21-479	178 (153)	33-582	0.0472

*indicates use of an unpaired t-test. All other comparison data were analyzed by Mann-Whitney test.

Table S6. Standardized pulmonary clinical history questionnaire used for the evaluation of clinical features of APECED pneumonitis in our study.

PNEUMONITIS SYMPTOM INTAKE FORM

1. CHRONIC OR RECURRENT COUGH

a) Age

b) Duration of cough episodes

c) Triggers

d) Frequency of episodes

e) Modifying factors

f) Dry yes/no

g) Productive yes/no

h) If both dry and productive at some point in time, what was the time sequence in which they manifested? (e.g., dry first for X number of years, then productive)

i) Any history of prolonged post infectious cough? yes/no
If so, how long does it last?

j) Sputum color

k) Sputum consistency

l) Sputum amount

m) Hemoptysis yes/no

n) Nocturnal symptoms yes/no

2. ASSOCIATED RESPIRATORY SYMPTOMS

Wheezing	yes/no
Dyspnea on exertion	yes/no
Dyspnea at rest	yes/no
Orthopnea	yes/no
Chest pain/tightness	yes/no
Fever	yes/no

3. **Previous h/o lung disease prior to diagnosis/previously labeled as:**
    a) Asthma yes/no
    b) Bronchitis yes/no
    c) Emphysema yes/no
    d) Pneumonia/recurrent pneumonias yes/no
    e) Other respiratory issues yes/no
    f) Sinus infections yes/no
    g) Ear infections yes/no

4. **Treatment history and response to initiation of treatment**

    Immune suppressive medication yes/no

    If yes, what medication and when was it started?

    Ongoing? yes

    Was there any improvement noted?

    If yes, what specifically?

    Frequency of bronchitis flares or exacerbations treated with antibiotics

    Any history of chronic antibiotics such as macrolides or inhaled antibiotics?

    If yes, details:

5. **Smoking status**
    Active smoker (pack per year)
    Never smoker
    Smoked but quit – symptoms improved after stopping?
    Passive smoking at home or work?

6. **Comments**

Table S7. Clinical, radiographic, lung biopsy, and autoantibody features of pneumonitis in the 21 affected patients with APECED included in this study.

Patient #	Chronic respiratory symptoms	Radiographic abnormalities	Lung biopsy	Bronchial tissue autoantibodies
1	Yes	Yes	Yes	Yes (BPIFB1; KCNRG)
2	Yes	Yes	No	Yes (BPIFB1)
3	Yes	Yes	No	No
4	Yes	Yes	No	Yes (BPIFB1)
5	Yes	Yes	Yes	Yes (BPIFB1)
6	Yes	Yes	Yes	Yes (BPIFB1)
7	Yes	Yes	No	Yes (BPIFB1)
8	Yes	Yes	Yes	Yes (BPIFB1; KCNRG)
9	Yes	Yes	Yes	Yes (BPIFB1; KCNRG)
10	Yes	Yes	No	Yes (BPIFB1)
11	Yes	Yes	No	Yes (BPIFB1)
12	Yes	Yes	Yes	Yes (BPIFB1; KCNRG)
13	Yes	Yes	Yes	No
14	Yes	Yes	No	Yes (BPIFB1)
15	Yes	Yes	Yes	Yes (BPIFB1)
16	Yes	Yes	Yes	Yes (BPIFB1)
17	Yes	Yes	No	No
18	Yes	Yes	Yes	No
19	Yes	Yes	Yes	Yes (KCNRG)
20	No	Yes	Yes	No
21	Yes	Yes	No	Yes (KCNRG)

BPIFB1, bactericidal/permeability-increasing fold-containing B1; KCNRG, potassium channel regulator.